Bioorganic & Medicinal Chemistry Letters 18 (2008) 4124–4129

Contents lists available at ScienceDirect

Bioorganic & Medicinal Chemistry Letters

journal homepage: www.elsevier.com/locate/bmcl

# Identification of novel non-peptide CXCR4 antagonists by ligand-based design approach

Satoshi Ueda [a], Manabu Kato [a], Shinsuke Inuki [a], Hiroaki Ohno [a], Barry Evans [b], Zi-xuan Wang [b], Stephen C. Peiper [b], Kazuki Izumi [c], Eiichi Kodama [c], Masao Matsuoka [c], Hideko Nagasawa [d], Shinya Oishi [a,*], Nobutaka Fujii [a,*]

[a] Graduate School of Pharmaceutical Sciences, Kyoto University, Sakyo-ku, Kyoto 606-8501, Japan
[b] Department of Pathology, Medical College of Georgia, GA 30912, USA
[c] Institute for Virus Research, Kyoto University, Sakyo-ku, Kyoto 606-8507, Japan
[d] Gifu Pharmaceutical University, Mitahora-higashi, Gifu 502-8585, Japan

ARTICLE INFO

*Article history:*
Received 6 April 2008
Revised 21 May 2008
Accepted 22 May 2008
Available online 29 May 2008

*Keywords:*
Chemokine
CXCR4
SDF-1
Anti-HIV
Indole

ABSTRACT

The design and synthesis of novel non-peptide CXCR4 antagonists is described. The peptide backbone of highly potent cyclic peptide-based CXCR4 antagonists was entirely replaced by an indole framework, which was expected to reproduce the disposition of the key pharmacophores consistent with those of potential bioactive conformations of the original peptides. A structure–activity relationship study on a series of modified indoles identified novel small-molecule antagonists having three pharmacophore functional groups through the appropriate linkers.



Chemokines are a family of small proteins with chemotactic and proactivatory effects on leukocytes. Chemokines mediate their biological effects by binding to the specific G-protein coupled receptor subtypes that are differentially and widely expressed in blood cells. Among these chemokine receptors, CXCR4 has a broad tissue distribution and the activation by its endogenous ligand CXCL12 (SDF-1, stromal cell-derived factor 1) leads to chemotaxis, immunomodulation, and other regulatory functions including progenitor cell migration during embryologic development of the cardiovascular, hematopoietic, and central nervous systems. In addition to its physiological roles, CXCR4 also plays important roles in pathological conditions. These include tumor growth and metastasis[1] and rheumatoid arthritis (RA).[2] CXCR4 has also been reported to act as a major co-receptor involved in the entry of T-cell-line-tropic human immunodeficiency virus type 1 (HIV-1) strains into target cells.[3] Thus, CXCR4 is considered as an important therapeutic target for multiple diseases. Inhibitory compounds of CXCL12 or HIV-1 binding to CXCR4 could be novel classes of anti-cancer, anti-RA, and anti-HIV-1 drugs. Previously, we found highly potent peptide-based CXCR4 antagonists such as **1**, **2**, and **3** (Fig. 1).[4,5]

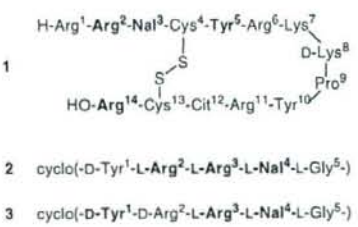


**Figure 1.** Structures of **1** and its downsized peptides **2** and **3**. Bold residues are the indispensable residues for the potent CXCR4-antagonistic activity. Nal, L-3-(2-naphthyl)alanine; Cit, L-citrulline.

Peptide **1** and its derivatives effectively blocked X4-HIV-1 entry to the cell by specifically binding to CXCR4,[6] and also showed an anti-metastatic effect against breast cancer[7] and anti-RA activity[8] in mouse models.

Although peptides are excellent lead molecules for development of pharmaceutical agents, special drug delivery systems are usually required for their clinical use because of the poor bioavailability and instability against enzymes. Whereas several peptide-based CXCR4 antagonists have been reported, only small numbers of small-molecule CXCR4 antagonists have been

* Corresponding authors. Tel.: +81 75 753 4551; fax: +81 75 753 4570 (N. Fujii).
*E-mail addresses:* soishi@pharm.kyoto-u.ac.jp (S. Oishi), nfujii@pharm.kyoto-u.ac.jp (N. Fujii).

0960-894X/$ - see front matter © 2008 Elsevier Ltd. All rights reserved.
doi:10.1016/j.bmcl.2008.05.092

reported.[9] These prompted us to design novel non-peptide CXCR4 antagonists based on the SAR and conformational studies on peptide ligands **1–3**.

Cyclic pentapeptide-based CXCR4 antagonists **2** and **3** were identified by screening of cyclic pentapeptide libraries, which were designed based on SAR studies of peptide **1**. The constrained backbone of the cyclic peptide was utilized as a template for positioning the key functional groups in space as is found in parent peptide **1**. Subsequent conformational analysis of **2** permitted us to determine the topology of the four indispensable residues, then, rational approach toward the de novo design of non-peptide antagonists may be envisaged.[10]

Our previous SAR studies on **2** and its derivatives have shown that at least three functional groups on the peptide side-chains are required: (1) an aromatic ring such as 2-naphthyl- or 3-indolyl group at position 4; (2) a guanidino group at position 3; (3) a guanidino group at position 2 or a phenol group at position 1.[11] However, it was difficult to determine the spatial relationships between these functional groups due to the free rotation of the side-chain torsion ($\chi$) angles. In our structural analyses, peptide **2** adopted a

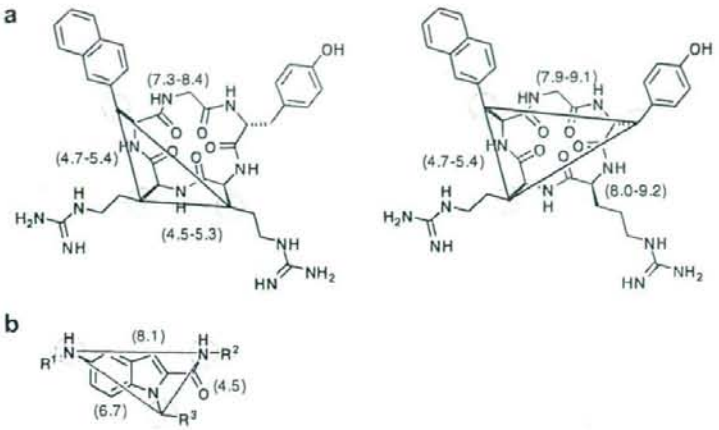


**Figure 2.** Design of indole-based CXCR4 antagonists based on molecular dynamics calculation of **2**. Distances (Å) between Cβ atoms bearing three essential functional groups during 1000 ps MD calculation of **2** (a) and between two key atoms of energy-minimized 5-acetamido-1-methylindole-2-carboxamide (b) are shown in parentheses. $R^1$–$R^3$ include naphthyl, indolyl, guanidino, and phenol groups.

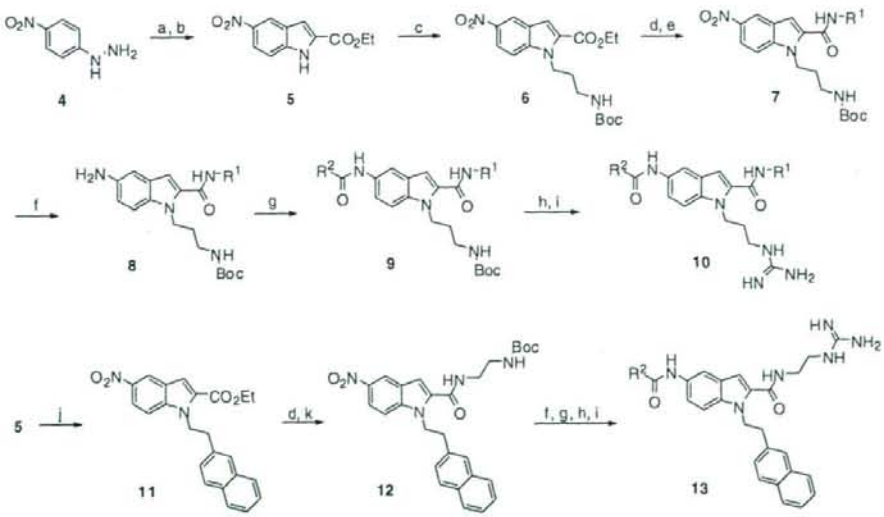


**Scheme 1.** Reagents and conditions; (a) ethyl pyruvate, EtOH, reflux; (b) polyphosphoric acid, xylene, 130 °C; (c) NaH, *N*-Boc-3-bromopropylamine, DMF, 70 °C; (d) 1 N NaOH aq., EtOH-THF; (e) $R^1$-$NH_2$, HATU, $Et_3N$, DMF; (f) $NH_4CO_2H$, Pd/C, EtOH-THF, reflux; (g) $R^2$-$CO_2H$, HATU, $Et_3N$, DMF; (h) 95% TFA-$H_2O$; (i) 1-*H*-pyrazolecarboxamidine hydrochloride, $Et_3N$, DMF; (j) 2-(2-naphthyl)ethyl bromide, NaH, DMF, 70 °C; (k) *N*-Boc-ethylenediamine, HATU, $Et_3N$, DMF.

variety of global conformations, in which the distances between indispensable functional groups were variable. On the other hand, relatively rigid cyclic peptide backbone and fixed distances between Cβ atoms, which append key functional groups, were observed.[5] Hence, we envisioned that introduction of crucial functional moieties for receptor binding onto a bicyclic heterocycle scaffold, which mimics the relatively fixed cyclic pentapeptide backbone of **2**, would provide non-peptide CXCR4 ligands. In this letter, we report a part of our ongoing research to develop novel non-peptide small molecule CXCR4 antagonists.

Among several molecular scaffold candidates, we first selected 5-aminoindole-2-carboxylic acid for the following reasons: (1) molecular modeling suggested that it met the spatial requirements for displaying the three key substituents (Fig. 2);[12] (2) accessible synthetic approaches were available for attachment of the three substituents; (3) indoles represent an important class of bioactive compounds and the physicochemical properties in terms of medicinal chemistry are well-documented.

Syntheses of indole-based compounds were achieved as shown in Scheme 1. (4-Nitrophenyl)hydrazine **4** was converted to the corresponding hydrazone, which was subjected to Fischer ring closure reaction to produce an indole **5**. Alkylation of $N^1$ position of the indole **5** with *N*-Boc-3-bromopropylamine gave **6**. This was hydrolyzed using 1 N aqueous sodium

**Table 1**
Inhibitory activities of indole derivatives **10a–j** and **13a–b** against binding of $^{125}$I-SDF-1α to CXCR4

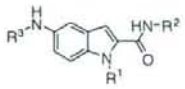

| Compound | $R^1$ | $R^2$ | $R^3$ | % inhibition at 10 μM |
|---|---|---|---|---|
| **10a** | 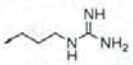 | 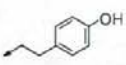 | 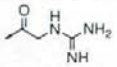 | 23 |
| **10b** | 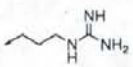 | 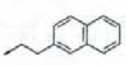 | 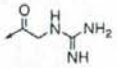 | 63 |
| **10c** | 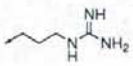 | 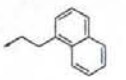 | 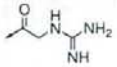 | 61 |
| **10d** | 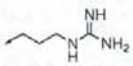 | 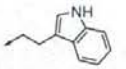 | 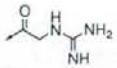 | 88 |
| **10e** | 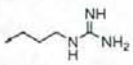 | 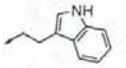 | 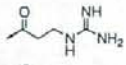 | 70 |
| **10f** | 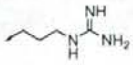 | 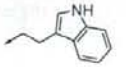 | 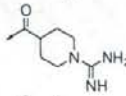 | 86 |
| **10g**[a] | 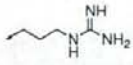 | 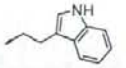 | 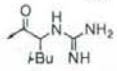 | 77 |
| **10h**[a] | 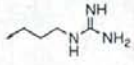 | 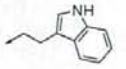 | 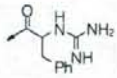 | 72 |
| **10i** | 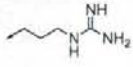 | 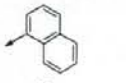 | 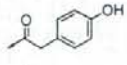 | 62 |
| **10j** | 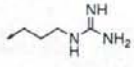 | 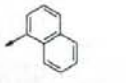 | 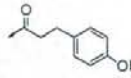 | 55 |
| **13a** | 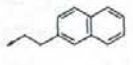 | 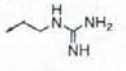 | 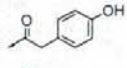 | 51 |
| **13b** | 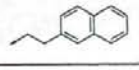 | 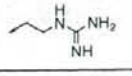 | 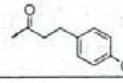 | 53 |

[a] Evaluated as a racemic mixture.

hydroxide in EtOH-THF and the resulting free carboxylic acid was coupled with amines using *O*-(7-azabenzotriazol-1-yl)-1,1,3,3-tetramethyluronium hexafluorophosphate (HATU) as coupling reagent to give **7**. The nitro group of **7** was reduced to amine **8** upon treatment with Pd-C and ammonium formate in EtOH. The aminoindole **8** was then coupled with carboxylic acids to give **9**. Deprotection of Boc group(s) by 95% TFA and guanylation of the free amino group(s) produced the target compounds **10**. Another series of compounds **13** were synthesized from **5** using similar reaction sequences described for **10**.

All indole-based compounds listed in Tables 1 and 2 were purified by preparative reverse-phase HPLC (purity >95%) and characterized by MALDI-TOF-MS. These compounds were tested for competitive binding inhibition in human CXCR4 transfected Chinese hamster ovary (CHO) cells using [$^{125}$I]SDF-1 as a radioligand, with the results given as percentage inhibition at 10 μM. $IC_{50}$ values of selected compounds are shown in Table 2.

Compound **10d** with 2-(3-indolyl)ethyl group at the $R^2$ position showed 88% inhibition at 10 μM ($IC_{50}$ = 3.0 μM) and was more potent than compounds having (4-hydroxyphenyl)-, (1-naphthyl)- or (2-naphthyl)-alkyl group at the $R^2$ position (compounds **10a–c**, 23–63% inhibition at 10 μM). Further SAR studies based on **10d** were undertaken. Chain elongation of the guanidinoacetyl group ($R^3$) of **10d** caused slight decrease in the affinity (**10e**). The use of *N*-amidinopiperidine-4-carbonyl was also acceptable for high potency [$IC_{50}$ (**10f**) = 3.0 μM]. Introduction of an isobutyl or benzyl group into the α-carbon of guanidinomethyl carbonyl group of **10d** did not cause significant drop in binding affinity (compounds **10g** and **10h**). Compounds with *S*-configuration at the chiral center showed more potent CXCR4 antagonistic activity as compared with the corresponding *R*-isomers. (***S***)-**10g** was identified as the most potent compound [$IC_{50}$ ((***S***)-**10g**) = 1.2 μM].[13] Compound (***S***)-**10g** also showed potent anti-HIV-1 activity (IIIB strain, inhibition of HIV-1 induced cytopathogenicity: $EC_{50}$ = 5.4 μM). The $IC_{50}$ value of (***S***)-**10g** is 34-fold lower as compared with parent peptide **2**. This is probably due to the absence of phenol functionality in (***S***)-**10g** which corresponds to D-Tyr side-chain of peptide **2**. Decreased number of amide bond in (***S***)-**10g** might also lead to the lower affinity. We have previously showed the importance of backbone amide functionalities of **2** for CXCR4 antagonistic activity by using reduced-amide isosteres or (*E*)-alkene dipeptide isosteres.[14]

Indole-based compounds having a phenol group at $R^3$ position showed moderate CXCR4-binding affinity (**10i**, **10j**, **13a**, and **13b**). Interestingly, these compounds did not show complete inhibition even at higher concentrations in the binding inhibition experiments, while compounds having a guanidino group at $R^3$ position (**10c**, **10d**, and (***S***)-**10g**) achieved complete inhibition (Fig. 3). These results suggest that **10c**, **10d** and (***S***)-**10g** are inhibitors that competitively bind to the SDF-1 binding site of CXCR4, while **10i**, **10j**, **13a**, and **13b** may bind to an allosteric site of CXCR4 and partially antagonize the SDF-1 binding.

Comparison of energy-minimized structures of (***S***)-**10g** and previously reported solution conformation of **2** revealed that three functional groups on the indole template well overlapped the three pharmacophore residues of **2** as expected. In this model, indole scaffold favorably mimicked the backbone of Arg–Arg–Nal sequence of **2** (see Fig. 4).

In summary, a series of indole-based compounds were designed, synthesized, and characterized as a novel class of CXCR4 antagonists. Although their $IC_{50}$ values are in the μM range, these indole derivatives could serve as a useful lead for further medicinal chemistry programs.

**Table 2**
$IC_{50}$ values of selected indole derivatives

| Compound | Structure | $IC_{50}$ (μM) |
|---|---|---|
| **10d** | 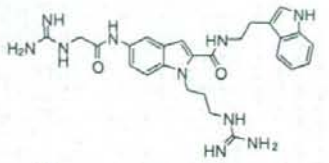 | 3.0 |
| **10f** | 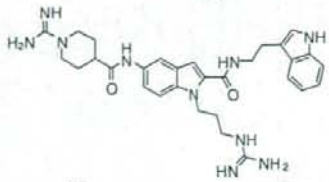 | 3.0 |
| (*S*)-**10g** | 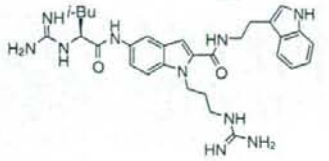 | 1.2 |
| (*R*)-**10g** | 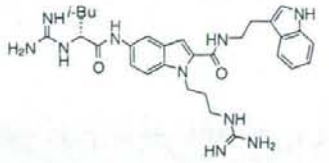 | 2.2 |
| (*S*)-**10h** | 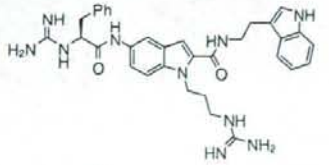 | 1.7 |
| (*R*)-**10h** | 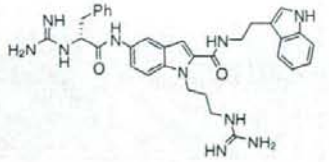 | 3.7 |
| **10i** | 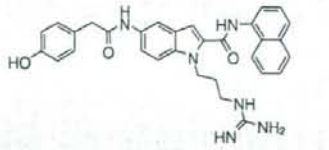 | 4.8 |
| **13b** | 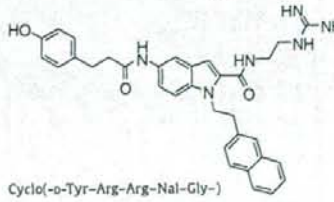 | 2.7 |
| **2** | Cyclo(-D-Tyr–Arg–Arg–Nal–Gly–) | 0.035 |

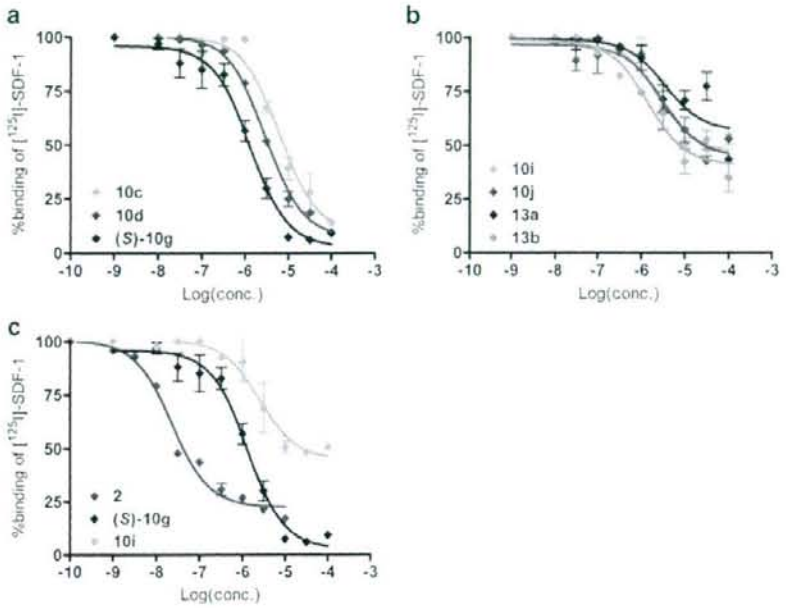


**Figure 3.** Ligand binding dose response of the compounds (a) having two guanidino pharmacophores and (b) having a phenol pharmacophore, and (c) the comparison of the two subsets with the parent peptide **2**.

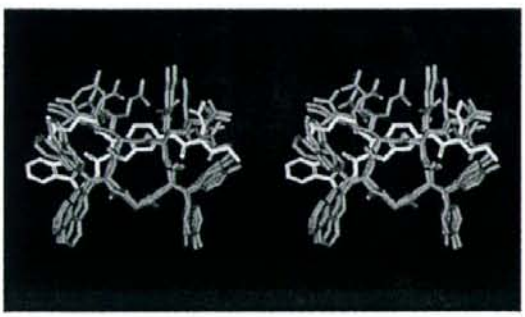

**Figure 4.** Overlay of a low-energy structure of (*S*)-**10g** (green) and **2** (gray). The molecular modeling of (*S*)-**10g** was performed using MacroModel-Program (Ver. 8.1) with 'MMFF' force field.


## Acknowledgments

This work was supported by Grant-in-Aid for Scientific Research and Targeted Proteins Research Program from the Ministry of Education, Culture, Sports, Science, and Technology of Japan, and Health and Labour Sciences Research Grants (Research on HIV/AIDS). Computation time was provided by the Supercomputer Laboratory, Institute for Chemical Research, Kyoto University. S.U. and S.I. are grateful to the JSPS Research Fellowships for Young Scientists.


## References and notes


1. Müller, A.; Homey, B.; Soto, H.; Ge, N.; Catron, D.; Buchanan, M. E.; Mcclanahan, T.; Murphy, E.; Yuan, W.; Wagner, S. M.; Barrera, J. L.; Mohar, A.; Verástegui, E.; Zlotnik, A. *Nature* **2001**, *410*, 50.
2. Nanki, T.; Hayashida, K.; El-Gabalawy, H. S.; Suson, S.; Shi, K.; Girschick, H. J.; Yavuz, S.; Lipsky, P. E. *J. Immunol.* **2000**, *165*, 6590.
3. Oberlin, E.; Amara, A.; Bachelerie, F.; Bessia, C.; Virelizier, J. L.; Arenzana-Seisdedos, F.; Schwartz, O.; Heard, J. M.; Clark-Lewis, I.; Legler, D. L.; Loetscher, M.; Baggiolini, M.; Moser, B. *Nature* **1996**, *382*, 833.
4. Masuda, M.; Nakashima, H.; Ueda, T.; Naba, H.; Ikoma, R.; Otaka, A.; Terakawa, Y.; Tamamura, H.; Ibuka, T.; Murakami, T.; Koyanagi, Y.; Waki, M.; Matsumoto, A.; Yamamoto, N.; Funakoshi, S.; Fujii, N. *Biochem. Biophys. Res. Commun.* **1992**, *189*, 845.
5. Fujii, N.; Oishi, S.; Hiramatsu, K.; Araki, T.; Ueda, S.; Tamamura, H.; Otaka, A.; Kusano, S.; Terakubo, S.; Nakashima, H.; Broach, J. A.; Trent, J. O.; Wang, Z.; Peiper, S. C. *Angew. Chem. Int. Ed.* **2003**, *42*, 3251.
6. Tamamura, H.; Xu, Y.; Hattori, T.; Zhang, X.; Arakaki, R.; Kanbara, K.; Omagari, A.; Otaka, A.; Ibuka, T.; Yamamoto, N.; Nakashima, H.; Fujii, N. *Biochem. Biophys. Res. Commun.* **1998**, *253*, 877.
7. (a) Tamamura, H.; Hori, A.; Kanzaki, N.; Hiramatsu, K.; Mizumoto, M.; Nakashima, H.; Yamamoto, N.; Otaka, A.; Fujii, N. *FEBS Lett.* **2003**, *550*, 79; (b) Takenaga, M.; Tamamura, H.; Hiramatsu, K.; Nakamura, N.; Yamaguchi, Y.; Kitagawa, A.; Kawai, S.; Nakashima, H.; Fujii, N.; Igarashi, R. *Biochem. Biophys. Res. Commun.* **2004**, *320*, 226.
8. Tamamura, H.; Fujisawa, M.; Hiramatsu, K.; Mizumoto, M.; Nakashima, H.; Yamamoto, N.; Otaka, A.; Fujii, N. *FEBS Lett.* **2004**, *569*, 99.
9. (a) Donzella, G. A.; Schols, D.; Lin, S. W.; Este, J. A.; Nagashima, K. A.; Maddon, P. J. *Nat. Med.* **1998**, *4*, 72; (b) Ichiya, K.; Yokoyama-Kumakura, S.; Tanaka, Y.; Tanaka, R.; Hirose, K.; Bannai, K.; Edamatsu, T.; Yanaka, M.; Niitani, Y.; Miyano-Kurosaki, N.; Takaku, H.; Koyanagi, Y.; Yamamoto, N. *Proc. Natl. Acad. Sci. U.S.A.* **2003**, *100*, 4185; (c) Tamamura, H.; Ojida, A.; Ogawa, T.; Tsutsumi, H.; Masuno, H.; Nakashima, H.; Yamamoto, N.; Hamachi, I.; Fujii, N. *J. Med. Chem.* **2006**, *49*, 3412; (d) Zhan, W.; Liang, Z.; Zhu, A.; Kurtkaya, S.; Shim, H.; Snyder, J. P.; Liotta, D. C. *J. Med. Chem.* **2007**, *50*, 5655.
10. Conversion of peptide to nonpeptide by scaffolding strategy, see: (a) Hirschmann, R.; Nicolaou, K. C.; Pietranico, S.; Salvino, J.; Leahy, E. M.; Sprengeler, P. A.; Furst, G.; Strader, C. D.; Cascieri, M. A.; Candelore, M. R.; Donaldson; Cindy; Vale, W.; Maechler, L. *J. Am. Chem. Soc.* **1992**, *114*, 9217; (b) Kawato, H. C.; Nakayama, K.; Inagaki, H.; Ohta, T. *Org. Lett.* **2001**, *3*, 3451; (c) Nakayama, K.; Kawato, H. C.; Inagaki, H.; Ohta, T. *Org. Lett.* **2001**, *3*, 3447.
11. (a) Ueda, S.; Oishi, S.; Wang, Z.-x.; Araki, T.; Tamamura, H.; Cluzeau, J.; Ohno, H.; Kusano, S.; Nakashima, H.; Trent, J. O.; Peiper, S. C.; Fujii, N. *J. Med. Chem.* **2007**, *50*, 192; (b) Tamamura, H.; Araki, T.; Ueda, S.; Wang, Z.; Oishi, S.; Esaka, A.; Trent, J. O.; Nakashima, H.; Yamamoto, N.; Peiper, S. C.; Otaka, A.; Fujii, N. *J. Med. Chem.* **2005**, *48*, 3280.
12. Distances (Å) between β-carbons of **2** during 1000 ps MD calculation; D-$Tyr^1$–$Arg^3$: 8.0–9.2, D-$Tyr^1$–$Nal^4$: 7.9–9.1, $Arg^3$–$Nal^4$: 4.7–5.4, $Arg^2$–$Arg^3$: 4.5–5.3, $Arg^2$–$Nal^4$: 7.3–8.4, $Arg^3$–$Nal^4$: 4.7–5.4. Distances (Å) between two key atoms of energy-minimized 5-acetamido-1-methylindole-2-carboxamide:

(acetamide N)-(*N*-methyl C), 6.7; (acetamide N)–(carboxamide N), 8.1; (methyl *C*)-(carboxamide N), 4.5.

13. Compound (*S*)-**10g**: $[\alpha]_D^{23}$ − 6.4(c0.35, $CH_3OH$); $^1H$ NMR (500 MHz, DMSO-$d_6$): $\delta$ = 0.93 (d, *J* = 6.0 Hz, 3H), 0.95 (d, *J* = 5.9 Hz, 3H), 1.60–1.76 (m, 3H), 1.92 (tt, *J* = 6.6, 7.2 Hz, 2H), 2.97 (t, *J* = 7.6 Hz, 2H), 3.14 (dt, *J* = 6.2, 6.6 Hz, 2H), 3.55 (dt, *J* = 6.7, 7.0 Hz, 2H), 4.26–4.41 (m, 1H), 4.55 (t, *J* = 7.2 Hz, 2H), 6.86–7.53 (brm, 8H), 6.99 (m, 1H), 7.03–7.11 (m, 2H), 7.20 (br, 1H), 7.33–7.43 (m, 2H), 7.55 (d, *J* = 9.0 Hz, 1H), 7.59 (d, *J* = 7.9 Hz, 1H), 7.73 (t, *J* = 5.4 Hz, 1H), 7.90 (d, *J* = 9.0 Hz, 1H), 7.95–7.99, (br, 1H), 8.65 (t, *J* = 5.7 Hz, 1H), 10.08 (s, 1H), 10.82 (s, 1H); LRMS (FAB): 573 ($MH^+$, base peak), 444; HRMS (FAB): calcd for $C_{30}H_{41}N_{10}O_2$ ($MH^+$) 573.3414; found 573.3418. Compound (*S*)-**10h**: $[\alpha]_D^{23}$ 3.3(c0.34, $CH_3OH$); $^1H$ NMR (500 MHz, DMSO-$d_6$): $\delta$ = 1.91 (tt, *J* = 7.2, 7.4 Hz, 2H), 2.96 (t, *J* = 7.3 Hz, 2H), 2.97–3.04 (m, 1H), 3.13 (dt, *J* = 5.4, 7.2 Hz, 2H), 3.20–3.27 (m, 1H), 3.54 (dt, *J* = 6.0, 7.3 Hz, 2H), 4.54 (t, *J* = 7.4 Hz, 2H), 4.56–4.62 (m, 1H), 6.78–7.64 (brm, 8H), 6.98 (m, 1H), 7.03–7.10 (m, 2H), 7.19 (m, 1H), 7.21–7.27 (m, 1H), 7.27–7.40 (m, 6H), 7.55 (d, *J* = 8.9 Hz, 1H), 7.58 (d, *J* = 7.7 Hz, 1H), 7.71 (t, *J* = 5.3 Hz, 1H), 7.85 (d, *J* = 8.9 Hz, 1H), 7.89–7.92, (br, 1H), 8.64 (t, *J* = 6.0 Hz, 1H), 10.12 (br, 1H), 10.82 (br, 1H); LRMS (FAB): 607 ($MH^+$, base peak), 444; HRMS (FAB): calcd for $C_{33}H_{39}N_{10}O_2$ ($MH^+$) 607.3257; found 607.3251.

14. Tamamura, H.; Hiramatsu, K.; Ueda, S.; Wang, Z.; Kusano, S.; Terakubo, S.; Trent, J. O.; Peiper, S. C.; Yamamoto, N.; Nakashima, H.; Otaka, A.; Fujii, N. *J. Med. Chem.* **2005**, *48*, 380.

CHEMBIOCHEM

DOI: 10.1002/cbic.200700761

# Synthesis and Application of Fluorescein- and Biotin-Labeled Molecular Probes for the Chemokine Receptor CXCR4

Shinya Oishi,*[a] Ryo Masuda,[a] Barry Evans,[b] Satoshi Ueda,[a] Yukiko Goto,[a] Hiroaki Ohno,[a] Akira Hirasawa,[a] Gozoh Tsujimoto,[a] Zixuan Wang,[b] Stephen C. Peiper,[b] Takeshi Naito,[c] Eiichi Kodama,[c] Masao Matsuoka,[c] and Nobutaka Fujii*[a]

*The design, synthesis, and bioevaluation of fluorescence- and biotin-labeled CXCR4 antagonists are described. The modification of D-Lys8 at an ε-amino group in the peptide antagonist Ac-TZ14011 derived from polyphemusin II had no significant influence on the potent binding of the peptide to the CXCR4 receptor. The application of the labeled peptides in flow cytometry and confocal microscopy studies demonstrated the selectivity of their binding to the CXCR4 receptor, but not to CXCR7, which was recently reported to be another receptor for stromal cell-derived factor 1 (SDF-1)/CXCL12.*

## Introduction

The CXC chemokine receptor 4 (CXCR4) is a G-protein-coupled cell-surface receptor that was identified previously as a coreceptor for infection by the T-cell-line-tropic (X4) human immunodeficiency virus type 1 (HIV-1).[1,2] Stromal cell-derived factor 1 (SDF-1)/CXCL12 is a homeostatic chemokine that regulates a number of physiological and pathologic processes through its interaction with and activation of CXCR4. SDF-1 secreted in bone-marrow stromal cells supports the retention of hematopoietic stem cells (HSCs), progenitor cells, and B-cell precursors in the hematopoietic microenvironment.[3] SDF-1 expression is implicated in the survival, growth, and development of CXCR4-expressing cells, including normal and malignant B lymphocytes, hematopoietic progenitors, and carcinoma cells.[3,4] It has also been demonstrated that concentration gradients of SDF-1 promote the homing of HSCs to bone marrow, the recruitment of progenitor cells to sites of ischemic tissue damage, and the metastasis of CXCR4-expressing neoplastic cells to target organs.[4,5]

Recently, CXCR7 (RDC1, CCX-CKR2) was reported to be another receptor for SDF-1.[6,7] CXCR7 promotes cell survival, growth, and adhesion in vitro and in vivo.[7,8] Furthermore, the expression pattern of CXCR7 is complementary to that of CXCR4 in the migrating primordium.[9,10] Therefore, the SDF-1–CXCR7 axis, like SDF-1–CXCR4, is relevant to the control processes of cell growth, migration, and recruitment. To investigate the distribution and localization of two binding partners of SDF-1, CXCR4 and CXCR7, both in vitro and in vivo, it would be useful to have access to selective and specific fluorescence- and otherwise-labeled ligands for these receptors.

To date, several CXCR4-receptor probes have been prepared and applied both in vitro[11–14] and in vivo.[15] Fluorescein-labeled SDF-1 was utilized to detect the CXCR4-dependent internalization of SDF-1 by stromal bone-marrow cells.[11] This labeled agonist was useful for evaluating the mechanism of receptor activation. We developed a potential radiopharmaceutical agent based on the polyphemusin II derived CXCR4 antagonist T140 (Scheme 1). Thus, [$^{111}$In]-diethylenetriaminepenta-

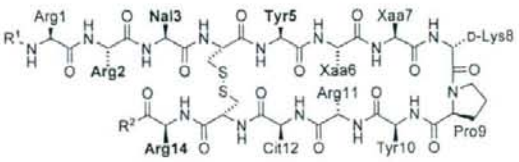


| | $R^1$ | $R^2$ | Xaa6 | Xaa7 |
|---|---|---|---|---|
| T140 | H | OH | Arg | Lys |
| Ac-TZ14011 (**1**) | Ac | $NH_2$ | Cit | Arg |

**Scheme 1.** Structure of the selective CXCR4 antagonists T140, which was used to design probe Ac-TZ14011 (**1**). Bold type indicates the pharmacophore residues.

[a] *Dr. S. Oishi, R. Masuda, Dr. S. Ueda, Y. Goto, Dr. H. Ohno, Dr. A. Hirasawa, Prof. Dr. G. Tsujimoto, Prof. Dr. N. Fujii*
*Graduate School of Pharmaceutical Sciences, Kyoto University*
*Sakyo-ku, Kyoto 606-8501 (Japan)*
*Fax: (+81) 75-753-4570*
*E-mail: soishi@pharm.kyoto-u.ac.jp*
*nfujii@pharm.kyoto-u.ac.jp*

[b] *B. Evans, Dr. Z. Wang, Prof. Dr. S. C. Peiper*
*Department of Pathology, Medical College of Georgia*
*Georgia 30912 (USA)*

[c] *T. Naito, Dr. E. Kodama, Prof. Dr. M. Matsuoka*
*Institute for Virus Research, Kyoto University*
*Sakyo-ku, Kyoto 606-8507 (Japan)*

*Supporting information for this article is available on the WWW under http://www.chembiochem.org or from the author.*

  

acetic acid (DTPA) labeled Ac-TZ14011 was designed for the in vivo imaging of CXCR4-expressing tumors.[15] Rhodamine-conjugated azamacrocycle antagonists were also developed; however, the small molecules were taken up into the cells by a potential active-transport process.[13]

On the basis of our previous research on peptide-based CXCR4 antagonists,[16] we conducted an extensive structure–activity-relationship analysis of labeled ligands with CXCR4 receptors expressed on the cell surface. Herein, we report the design of the labeled antagonists and their application in in vitro experiments, including flow cytometry. The selectivity of the ligand for CXCR4 versus CXCR7 was also investigated by confocal microscopy.

## Results and Discussion

### Peptide design and synthesis

Previous alanine-scanning experiments identified four indispensable pharmacophore residues of T140, which are located peripheral to the disulfide bridge.[17] On the other hand, modification of the N and C termini or β-turn region with several types of functional groups or peptidomimetics did not lead to a decrease in activity.[16] For example, arylacyl functional groups, such as fluorobenzoyl, at the N terminus of T140 analogues enhanced anti-HIV activity.[18] On the basis of these precedent structure–activity-relationship studies on T140 derivatives, we designed two types of potential labeled CXCR4 ligands (Tables 1 and 2). The functional groups for labeling were attached with an appropriate spacer by acylation to the α-amino group of the N-terminal Arg1 residue or on the ε-amino group of D-Lys8. To identify appropriate fluorophores that did not affect peptide binding affinity to CXCR4, carboxyfluorescein and Alexa Fluor 488, which have a similar fluorescence spectrum, were used for fluorescence labeling. The different functional groups on the fluorescent section of peptides could have an effect on the affinities of the peptides for CXCR4. The Alexa Fluor 488 dye, which contains an amino group, an imino group, and two sulfonate groups on a xanthene structure, exhibited greater photostability and pH insensitivity.

**Table 1.** Sequences and biological activity of labeled T140 analogues.

R-Arg-Arg-Nal-Cys-Tyr-Cit-Arg-D-**Xaa**-Pro-Tyr-Arg-Cit-Cys-Arg-$NH_2$

| Peptide | R | D-Xaa | $IC_{50}$ [nM][a] |
|---|---|---|---|
| 1 | Ac | D-Lys | 5.2 ± 0.1 |
| 2 | Ac | D-Glu | 6.7 ± 2.6 |
| 3 | fluorescein | D-Lys | 24 ± 0.3 |
| 4 | fluorescein | D-Glu | 199 ± 26 |
| 5 | Alexa Fluor 488 | D-Glu | 5700 ± 769 |

[a] $IC_{50}$ values for the peptides are based on the inhibition of [$^{125}$I]SDF-1 binding to CHO cells that were transfected with CXCR4.

**Table 2.** Sequences and biological activity of Ac-TZ14011 analogues.

Ac-Arg-Arg-Nal-Cys-Tyr-Cit-Arg-D-**Lys**(R)-Pro-Tyr-Arg-Cit-Cys-Arg-$NH_2$

| Peptide | R | $IC_{50}$ [nM][a] |
|---|---|---|
| 1 | H (amine) | 5.2 ± 0.1 |
| 6 | fluorescein | 16 ± 0.8 |
| 7 | fluorescein-Acp- | 26 ± 2.4 |
| 8 | biotin-Acp- | 11 ± 0.1 |
| 9 | Alexa Fluor 488 | 8.1 ± 3.5 |
| 10 | Alexa Fluor 488-Acp- | 267 ± 19 |

[a] $IC_{50}$ values for the peptides are based on the inhibition of [$^{125}$I]SDF-1 binding to CHO cells that were transfected with CXCR4.

Peptide resins were constructed manually by standard Fmoc-based solid-phase peptide synthesis (SPPS) by using *N,N'*-diisopropylcarbodiimide (DIC)/1-hydroxybenzotriazole (HOBt). Fluorescein or acetyl modification at the N-terminal α-amino group of peptides **1–4** was carried out on the resin by using carboxyfluorescein/DIC/HOBt or $Ac_2O$/pyridine, respectively. For the preparation of peptides **6–8** and **10** with either a fluorescein label or a 6-aminocaproic acid (Acp) linker combined with a fluorescein, biotin, or Alexa Fluor 488 label on the ε-amino group of D-Lys8, a 4-methyltrityl (Mtt) group was used for side-chain protection (Scheme 2). After the removal of the Mtt group on peptide **11** with 1,1,1,3,3,3-hexafluoropropan-2-ol (HFIP), an Acp linker and/or labeling groups were attached to the peptide resin **12** by a standard protocol to afford the labeled protected peptide resins **13–16**. Treatment of the protected peptide resins with TFA/1,2-ethanedithiol (EDT)/$H_2O$ (95:2.5:2.5) followed by air oxidation in aqueous solution yielded the expected peptides **1–4**, **6–8**, and **17**.

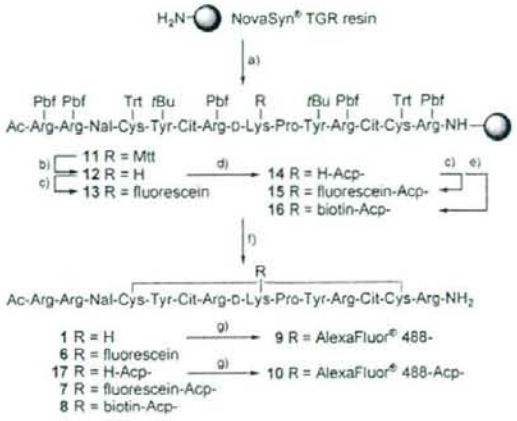


**Scheme 2.** Synthesis of D-Lys8-labeled CXCR4 antagonists: a) Fmoc-based peptide synthesis; b) $CH_2Cl_2$/HFIP/TFE/TES (65:20:10:5); c) carboxyfluorescein, DIC, HOBt; d) Fmoc-Acp-OH, DIC, HOBt, then 20% piperidine/DMF; e) biotin, DIC, HOBt; f) TFA/EDT/$H_2O$ (95:2.5:2.5), then $NH_4OH$; g) Alexa Fluor 488–OSu, $iPr_2NEt$. DMF: *N,N*-dimethylformamide; Fmoc: 9-fluorenylmethoxycarbonyl; Pbf: 2,2,4,6,7-pentamethyldihydrobenzofuran-5-sulfonyl; TFE: 2,2,2-trifluoroethanol; TES: triethylsilane; Trt: triphenylmethyl (trityl).

Labeling with Alexa Fluor 488 was performed with the activated succinimidyl ester, which is commercially available. The

  

precursor peptides (e.g., **1**, **17**) were modified in DMF to provide the expected peptides **5**, **9**, and **10** with a single Alexa Fluor 488 dye moiety.[19]

### Biological evaluation of fluorescein- and biotin-labeled peptides

The CXCR4-antagonistic activity of peptides **1–10** was evaluated with respect to the inhibition of [$^{125}$I]SDF-1 binding to CXCR4 Chinese hamster ovary (CHO) cell transfectants. The replacement of D-Lys8 in the parent peptide **1** with D-glutamic acid had no significant effect on the bioactivity of the peptide ($IC_{50}$(**1**) = 5.2 nM; $IC_{50}$(**2**) = 6.7 nM; Table 1); this is consistent with the results of previous Glu-scanning experiments of a related peptide.[20] This result suggested that the modification of the β turn $i+1$ position of the peptides with a functional group for labeling would be possible. Fluorescein modification of the N terminus of peptides **1** and **2** led to a slight and significant decrease in inhibitory activity ($IC_{50}$(**3**) = 24 nM; $IC_{50}$(**4**) = 199 nM), respectively. Although the substituted benzoyl and pyridinecarbonyl groups at the N terminus of the peptide improved its bioactivity,[18] an additional xanthene or carboxyl group might be unfavorable to ligand binding with CXCR4. The Alexa Fluor 488 labeled peptide **5** showed a significant decrease in inhibitory activity ($IC_{50}$(**5**) = 5.7 μM); this indicates that the N terminus is inappropriate for fluorescence labeling.

Modification of the ε-amino group of D-Lys8 in the parent peptide **1** was another promising approach to the creation of labeled CXCR4 antagonists (Table 2). The fluorescein-modified peptides **6** and **7** exhibited slightly decreased bioactivity but retained significant binding affinity for CXCR4 ($IC_{50}$(**6**) = 16 nM; $IC_{50}$(**7**) = 26 nM). The biotin-labeled peptide **8** containing an Acp spacer, which would be helpful for the simultaneous binding of **8** with CXCR4 and avidins, was also a potent inhibitor ($IC_{50}$(**8**) = 11 nM). Thus, the presence of a functional group at this position for labeling, with or without an Acp spacer, did not appear to influence the bioactivity of the peptide. We concluded that the D-Lys8 residue in the β-turn region might be unimportant for direct molecular recognition by CXCR4; consequently, this position was considered to be more appropriate for labeling. The Alexa Fluor 488 labeled peptide **9** without an Acp linker showed nearly equipotent inhibitory activity to that of the parent peptide **1** ($IC_{50}$(**9**) = 8.1 nM). In contrast, significantly lower bioactivity was observed for peptide **10**, which contains an Acp linker ($IC_{50}$(**10**) = 267 nM). This result implies that the modified xanthene structure of Alexa Fluor 488 might cause some unfavorable interactions with the receptor, contrary to our expectations. The two potent labeled peptides **6** and **9** were used for further experiments.

### Application of fluorescence-labeled peptides to flow cytometry and confocal microscopy studies

The applicability of the fluorescence-labeled CXCR4 antagonists **6** and **9** to in vitro experiments was investigated (Figure 1A and B). CHO cells that expressed high levels of the CXCR4 receptor and CXCR4-negative control cells were incubated with peptide **6** or **9** (200 nM), and the resulting mixtures were analyzed by flow cytometry. The CXCR4-expressing cells bound the fluorescent ligand, but the cells that did not express CXCR4 were not stained. The binding of peptides **6** and **9** was inhibited by competition with the unlabeled specific CXCR4 antagonist T140 (200 nM). This result supports the specificity of the fluorescent ligands for CXCR4. With the fluorescent probe **6**, lymphocytes derived from mouse spleen were identified by light scatter gating and analyzed for binding of the fluorescent antagonists (Figure 1C). Peptide **6** bound to CXCR4-expressing lymphocytes, and the staining was inhibited competitively by the addition of unlabeled T140 (200 nM). Peptide **6** was also utilized for the detection of chemotactic cells in a transmigration assay with CXCL12 (Figure 1D). Whereas a low percentage of the cells in the top well of a chemotaxis chamber were positive, the cells which passed through 3-μm pores in response to the CXCL12 chemotactic gradient were all stained positively with peptide **6**.

The probing ability of **6** and **9** for CXCR4 was also verified by confocal microscopy studies on CXCR4-expressing HEK293 cells (Figure 2). The cell surface of CXCR4-positive cells was stained with peptides **6** and **9** in a dose-dependent manner (Figure 2A; see also the Supporting Information). This result is in contrast to a previous report that a rhodamine-labeled azamacrocycle localizes in the cytoplasm by nonspecific uptake.[13] Staining was not observed with CXCR4-negative control cells; this suggests that receptor recognition of these fluorescent peptides is specific to CXCR4 (Figure 2C). Furthermore, CXCR7-expressing HEK293 cells were not stained by the fluorescent peptides **6** and **9** (Figure 2B); this indicates that these T140 derivatives are selective inhibitors of the CXCR4 receptor.

## Conclusions

In the current study the effects of labeling a peptide at different positions with various functionalities with a view to retaining indispensable interactions with the CXCR4 receptor was investigated. Fluorescein, biotin, and Alexa Fluor 488 moieties on the D-Lys8 ε-amino group of the parent peptide were appropriate labels. The resulting labeled peptides exhibited specific and high affinity for the CXCR4 receptor, but not for the CXCR7 receptor. The labeled peptides could be useful as selective molecular probes for the CXCR4 receptor in future in vitro and/or in vivo experiments.

## Experimental Section

**General procedure for peptide synthesis:** Protected peptide resins were constructed manually by standard Fmoc-based SPPS on NovaSyn TGR resin (192 mg, 0.05 mmol) by using DIC (39 μL, 0.25 mmol) in combination with HOBt (38 mg, 0.25 mmol). The side chains Tyr, Glu, Lys, Cys, and Arg were protected with *t*Bu, *t*Bu ester, Boc, Trt, and Pbf groups, respectively. For the preparation of peptides **6–8** and **10**, the Mtt group was used to protect the D-Lys8 side chain. The N-terminal α-amino group was acetylated by treatment of the resin with $Ac_2O$ (24 μL, 0.25 mmol) and pyridine (40 μL, 0.10 mmol). Biotin (61 mg, 0.25 mmol) or carboxyfluorescein (94 mg, 0.25 mmol) was coupled to the peptide by using DIC

  

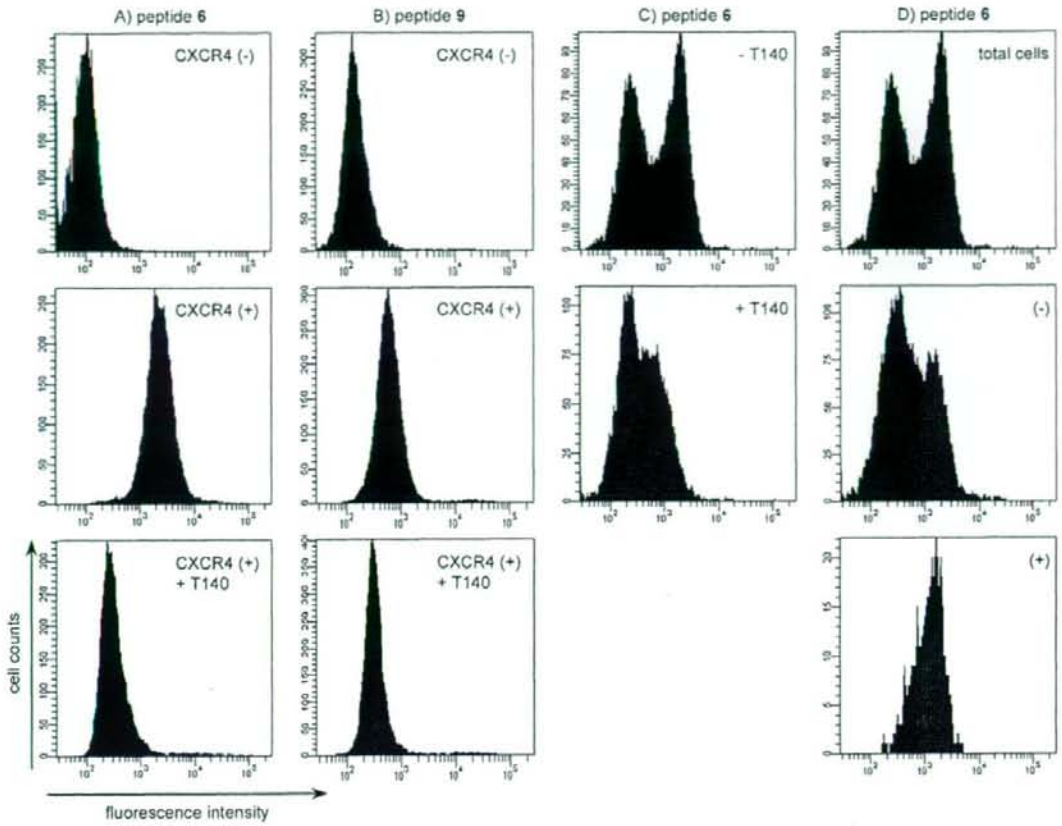


**Figure 1.** Application of fluorescent CXCR4 antagonists **6** and **9** to flow cytometry. CHO cells were incubated with labeled peptides (200 nM) A) **6**, and B) **9**. The top and middle panels show the results with cells that did not (−) and did express CXCR4 (+), respectively. Competitive binding was assessed with T140 (200 nM; lower panels). C) FACS (fluorescence-activated cell sorting) data for mouse spleen cells treated with peptide **6** (200 nM) in the presence (+) and absence (−) of T140 (200 nM). D) Chemotaxis experiment with mouse spleen cells (top panel). Cells from the total population that did not display chemotaxis are shown in the middle panel (−), and cells that migrated in response to a gradient of SDF-1 are shown in the lower panel (+).

(39 μL, 0.25 mmol) and HOBt (38 mg, 0.25 mmol) in DMF (2 mL). The resulting protected peptide resin (0.05 mmol) was treated with TFA/$H_2O$/EDT (95:2.5:2.5, 4 mL) for 2 h at room temperature. After removal of the resin by filtration, ice-cold dry $Et_2O$ (100 mL) was added to the residue. The resulting powder was collected by centrifugation and then washed with ice-cold dry $Et_2O$ (3×50 mL). The crude reduced peptide was dissolved in $H_2O$ (100 mL), and the pH value was adjusted to 8.0 with $NH_4OH$. After oxidation by exposure to air for 1 day, the crude product in the solution was purified by preparative HPLC to afford the desired peptide as a white powder.

**Removal of the Mtt protecting group**: The resin (0.05 mmol) was treated with $CH_2Cl_2$/HFIP/TFE/TES (6.5:2:1:0.5, 10 mL) for 2 h at room temperature. It was then washed with the same mixture twice, treated with 10% $iPr_2NEt$ in DMF, and used for the next coupling.

**Conjugation of Alexa Fluor 488 succinimidyl ester with peptides**: Lyophilized peptide (4.66 μmol) and $iPr_2NEt$ (3.77 μL, 27.2 μmol) were added to a solution of Alexa Fluor 488 succinimidyl ester (2.50 mg, 3.88 μmol) in DMF (250 μL), and the resulting mixture was stirred in the dark for 12 h at room temperature. The crude mixture was then diluted with MeOH (100 μL) and purified by HPLC. Fractions containing Alexa Fluor 488 conjugates were collected and lyophilized to give **5** (3.3 mg, 27%), **9** (5.1 mg, 51% from **1**), or **10** (5.88 mg, 46% from **17**) as a red powder.

## Acknowledgements

*This research was supported by a Grant-in-Aid for Scientific Research from the Ministry of Education, Culture, Sports, Science, and Technology of Japan, the 21st Century COE Program "Knowledge Information Infrastructure for Genome Science", and the Targeted Proteins Research Program. S.U. is grateful for a JSPS Research Fellowship for Young Scientists. We thank Maxwell Reback (Kyoto University) for reading the manuscript.*

  

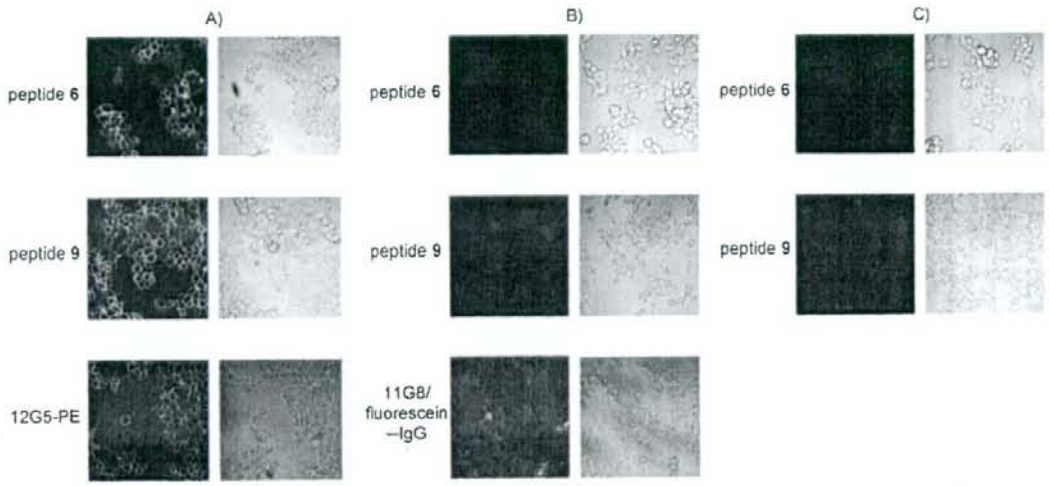


**Figure 2.** Confocal images of HEK293 cells stained with peptides **6** and **9** (100 nM): A) CXCR4-expressing cells, B) CXCR7-expressing cells, C) CXCR4-negative control cells. CXCR4- and CXCR7-receptor expression was verified by using the monoclonal antibodies 12G5 and 11G8.

**Keywords:** cell imaging · chemokine receptors · CXCR4 antagonists · fluorescent probes · peptides

[1] Y. Feng, C. C. Broder, P. E. Kennedy, E. A. Berger, *Science* **1996**, *272*, 872–877.
[2] E. Oberlin, A. Amara, F. Bachelerie, C. Bessia, J. L. Virelizier, F. Arenzana-Seisdedos, O. Schwartz, J. M. Heard, I. Clark-Lewis, D. F. Legler, M. Loetscher, M. Baggiolini, B. Moser, *Nature* **1996**, *382*, 833–835.
[3] T. Nagasawa, *Nat. Rev. Immunol.* **2006**, *6*, 107–116.
[4] J. A. Burger, T. J. Kipps, *Blood* **2006**, *107*, 1761–1767.
[5] T. Lapidot, A. Dar, O. Kollet, *Blood* **2005**, *106*, 1901–1910.
[6] K. Balabanian, B. Lagane, S. Infantino, K. Y. Chow, J. Harriague, B. Moepps, F. Arenzana-Seisdedos, M. Thelen, F. Bachelerie, *J. Biol. Chem.* **2005**, *280*, 35760–35766.
[7] J. M. Burns, B. C. Summers, Y. Wang, A. Melikian, R. Berahovich, Z. Miao, M. E. Penfold, M. J. Sunshine, D. R. Littman, C. J. Kuo, K. Wei, B. E. McMaster, K. Wright, M. C. Howard, T. J. Schall, *J. Exp. Med.* **2006**, *203*, 2201–2213.
[8] Z. Miao, K. E. Luker, B. C. Summers, R. Berahovich, M. S. Bhojani, A. Rehemtulla, C. G. Kleer, J. J. Essner, A. Nasevicius, G. D. Luker, M. C. Howard, T. J. Schall, *Proc. Natl. Acad. Sci. USA* **2007**, *104*, 15735–15740.
[9] C. Dambly-Chaudière, N. Cubedo, A. Ghysen, *BMC Dev. Biol.* **2007**, *7*, 23.
[10] G. Valentin, P. Haas, D. Gilmour, *Curr. Biol.* **2007**, *17*, 1026–1031.
[11] A. Dar, P. Goichberg, V. Shinder, A. Kalinkovich, O. Kollet, N. Netzer, R. Margalit, M. Zsak, A. Nagler, I. Hardan, I. Resnick, A. Rot, T. Lapidot, *Nat. Immunol.* **2005**, *6*, 1038–1046.
[12] O. Kollet, A. Dar, S. Shivtiel, A. Kalinkovich, K. Lapid, Y. Sztainberg, M. Tesio, R. M. Samstein, P. Goichberg, A. Spiegel, A. Elson, T. Lapidot, *Nat. Med.* **2006**, *12*, 657–664.
[13] A. Khan, J. D. Silversides, L. Madden, J. Greenman, S. J. Archibald, *Chem. Commun.* **2007**, 416–418.
[14] W. Zhan, Z. Liang, A. Zhu, S. Kurtkaya, H. Shim, J. P. Snyder, D. C. Liotta, *J. Med. Chem.* **2007**, *50*, 5655–5664.
[15] H. Hanaoka, T. Mukai, H. Tamamura, T. Mori, S. Ishino, K. Ogawa, Y. Iida, R. Doi, N. Fujii, H. Saji, *Nucl. Med. Biol.* **2006**, *33*, 489–494.
[16] H. Tsutsumi, T. Tanaka, N. Ohashi, H. Masuno, H. Tamamura, K. Hiramatsu, T. Araki, S. Ueda, S. Oishi, N. Fujii, *Biopolymers* **2007**, *88*, 279–289.
[17] H. Tamamura, A. Omagari, S. Oishi, T. Kanamoto, N. Yamamoto, S. C. Peiper, H. Nakashima, A. Otaka, N. Fujii, *Bioorg. Med. Chem. Lett.* **2000**, *10*, 2633–2637.
[18] H. Tamamura, K. Hiramatsu, M. Mizumoto, S. Ueda, S. Kusano, S. Terakubo, M. Akamatsu, N. Yamamoto, J. O. Trent, Z. Wang, S. C. Peiper, H. Nakashima, A. Otaka, N. Fujii, *Org. Biomol. Chem.* **2003**, *1*, 3663–3669.
[19] The fluorescent peptides **3–7**, **9**, and **10** contain the fluorescent labels in two regioisomeric forms derived from commercially available carboxyfluorescein and Alexa Fluor 488 succinimidyl ester.
[20] H. Tamamura, K. Hiramatsu, S. Kusano, S. Terakubo, N. Yamamoto, J. O. Trent, Z. Wang, S. C. Peiper, H. Nakashima, A. Otaka, N. Fujii, *Org. Biomol. Chem.* **2003**, *1*, 3656–3662.

Received: December 15, 2007
Published online on April 15, 2008

  

Antiviral Research 80 (2008) 71–76

Contents lists available at ScienceDirect

Antiviral Research

journal homepage: www.elsevier.com/locate/antiviral

# Novel screening systems for HIV-1 fusion mediated by two extra-virion heptad repeats of gp41

Hiroki Nishikawa[a], Eiichi Kodama[b,*], Ayako Sakakibara[b], Ayako Fukudome[b], Kazuki Izumi[b], Shinya Oishi[a], Nobutaka Fujii[a], Masao Matsuoka[b]

[a] Graduate School of Pharmaceutical Sciences, Kyoto University, Sakyo-ku, Kyoto 606-8501, Japan
[b] Laboratory of Virus Immunology, Institute for Virus Research, Kyoto University, Sakyo-ku, Kyoto 606-8507, Japan

ARTICLE INFO

*Article history:*
Received 12 November 2007
Accepted 5 May 2008

*Keywords:*
HIV-1
Gp41
Fusion
ELISA
Screening
Alkaline phosphatase

ABSTRACT

Entry of human immunodeficiency virus type 1 (HIV-1) into target cells is mediated by its envelope protein gp41 through membrane fusion. Interaction of two extra-virion heptad repeats (HRs) in the gp41 plays a pivotal role in the fusion, and its inhibitor, enfuvirtide (T-20), blocks HIV-1 entry. To identify agents that block HIV-1 fusion, two screening methods based on detection and quantification by the enzyme-linked immunosorbent assay (ELISA) principle have been established. One method uses an alkaline phosphatase (ALP)-conjugated antibody (Ab-ELISA) and the other uses an ALP-fused HR (F-ELISA) to detect and quantify the interaction of the two HRs. The F-ELISA was more simple and rapid, since no ALP-conjugated antibody reaction was required. Both ELISAs detected all the fusion inhibitors tested except for T-20. Interaction of the two HRs was observed in both ELISAs, even in the presence of 10% dimethyl sulfoxide. Ab-ELISA performed best in a pH ranging from 6 to 8, while F-ELISA performed best at a pH ranging from 7 to 8. These results indicate that both established ELISAs are suitable for the identification of HIV-1 fusion inhibitors.



## 1. Introduction

Combination chemotherapy has been widely used and reduces the mortality caused by HIV-1 infection. During prolonged therapy, however, in some patients, such efficacy is attenuated by the emergence of drug-resistant variants (Calmy et al., 2004). Moreover, combination chemotherapy occasionally induces various adverse effects and may also increase the costs of the therapy. Therefore, development of novel anti-HIV-1 drugs that suppress replication of resistant variants, and are less toxic and less cost is urgently needed.

There are at least two approaches to controlling replication of resistant variants and/or to reducing unfavorable adverse effects induced by the therapy. One approach is the development of anti-HIV-1 drugs which inhibit new targets such as viral integrase (Hazuda et al., 2004) or cellular receptors such as CCR5 (Tagat et al., 2004). Actually, an integrase inhibitor, raltegravir (Grinsztejn et al., 2007), and a CCR5 antagonist, maraviroc (Fätkenheuer et al., 2005) have been approved for clinical application. The other is the development or modification of current drugs that inhibit well-established targets, to make them effective against resistant variants while reducing adverse side-effects. In this study, we focus on the recently established and promising target of virus–cell membrane fusion.

The mechanism of virus–cell membrane fusion has already been disclosed (Eckert and Kim, 2001). Briefly, one of the HIV-1 envelope glycoproteins, gp120, binds to the host cell receptor CD4 and CXCR4 or CCR5, and then, another membrane-spanning protein gp41 in trimer anchors itself to the host cell membrane. After anchoring, heptad repeats 1 and 2 (HR1 and HR2), which are two extra-virion α-helical regions in the gp41, form an anti-parallel 6-helical bundle and lead to fusion of HIV-1 with the host cell membrane. On the basis of this molecular mechanism, compounds which prevent 6-helical bundle formation will be potential HIV-1 fusion inhibitors. Enfuvirtide (T-20) is the first peptide approved and used against HIV-1 variants that are refractory to the effect of reverse transcriptase and protease inhibitors (Lalezari et al., 2003; Lazzarin et al., 2003). Previously, we and others have developed novel potent fusion inhibitors, in the form of gp41 HR2-derived peptides (Bewley et al., 2002; Otaka et al., 2002; Root et al., 2001) (Fig. 1) and small molecules (Cai and Gochin, 2007; Frey et al., 2006). However, no fusion inhibitors, except for T-20, have been approved for clinical use. To screen further potential fusion inhibitors, we have established two simple, rapid and reproducible

* Corresponding author. Tel.: +81 75 751 3986; fax: +81 75 751 3986.
*E-mail address:* ekodama@virus.kyoto-u.ac.jp (E. Kodama).

0166-3542/$ – see front matter © 2008 Elsevier B.V. All rights reserved.
doi:10.1016/j.antiviral.2008.05.006

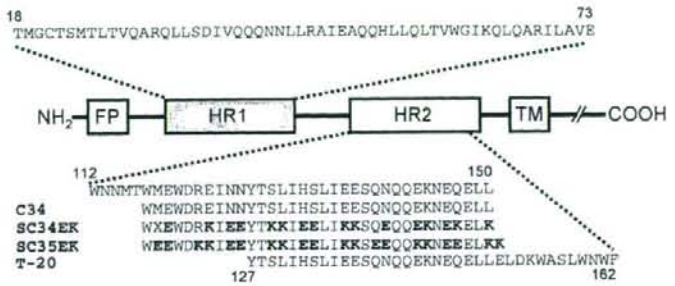


**Fig. 1.** Schematic view of gp41. The locations of the fusion peptide (FP), N-terminal heptad repeat region (HR1), C-terminal heptad repeat region (HR2), transmembrane domain (TM) and amino acid sequence of HR1, HR2, T-20, C34 and its derivatives (Otaka et al., 2002) are shown. The residue numbers of each peptide correspond to their positions in the envelope protein gp41 of HIV-1 NL4-3 clone. Representative regions of HR1 and HR2 used in this study are defined by the amino acids 18–73 and 112–150, respectively, and designated as MBP-HR1- and GST-HR2- or TRX-ALP-HR2-fused protein as described in Section 2. The X in SC34EK indicates an artificial amino acid norleucine instead of methionine, to avoid oxidation of the methionine residue.

in vitro screening systems using the enzyme-linked immunosorbent assay (ELISA).

## 2. Materials and methods

### 2.1. Antiviral agents

The peptide-based fusion inhibitors were synthesized as described previously (Otaka et al., 2002), and their sequences are shown in Fig. 1. CCR5 antagonist TAK-779 (Baba et al., 1999) was provided by Takeda Pharmaceutical Company Ltd. (Osaka, Japan) through an AIDS research and reference reagent program. CXCR4 antagonist AMD-3100 (De Clercq et al., 1994) was provided by S. Shigeta (Fukushima Medical University, Fukushima, Japan). Adsorption inhibitor dextran sulfate MW 5000, DS-5000 (Baba et al., 1988) was purchased from Sigma (St. Louis, MO).

### 2.2. Protein expression and purification

A DNA fragment of the alkaline phosphatase (ALP) coding region without its secretory signal sequence, corresponding to amino acids 22–471 (Dodt et al., 1986; Kikuchi et al., 1981), was amplified by PCR from the *E. coli* JM109 genome (K12 strain; GenBank accession number: U00096). The amplified ALP region was ligated into the pET32a vector (Novagen, Madison, WI) to create pET32-ALP, a thioredoxin (TRX)-ALP fusion construct. A DNA fragment coding the HR1 region of HIV-1 gp41, amino acid positions 18–73, was amplified by PCR from an HIV-1 molecular clone pNL4-3 (GenBank accession number: AF324493). The amplified HR1 region was ligated into the pMAL-C2 vector (New England Biolabs, Ipswich, MA) to express HR1 with maltose-binding protein (MBP) as a tag, designated pMAL-HR1. The HR2 region, gp41 amino acid positions 112–150, was also amplified and ligated into both the pGEX-5X vector (GE Healthcare, Buckinghamshire, UK) and the pET32-ALP construct to express HR2 fusion protein with glutathione *S*-transferase (GST) and TRX-ALP, designated pGEX-HR2 and pET32-ALP-HR2, respectively. All vectors were verified by DNA sequencing and transformed into *E. coli* BL21-CodonPlus (DE3)-RIL strain (Stratagene, La Jolla, CA) for bacterial expression. The expressed MBP-HR1, GST-HR2 and TRX-ALP-HR2 proteins were purified by Amylose Resin (New England Biolabs), Glutathione Sepharose 4B (GE Healthcare) and Ni-NTA Agarose (Qiagen, Valencia, CA), respectively, according to the Manufacturers' recommended protocols. Purity was determined by SDS–PAGE and concentration by the Bradford protein assay (Bio-Rad, Hercules, CA).

### 2.3. Indirect detection of interaction of HR1 and HR2 (Ab-ELISA) (Fig. 2A)

Fifty nanomolar MBP-HR1 dissolved in 50 mM sodium carbonate buffer (pH 9.4) was coated on a 96-well ELISA plate (Costar, Cambridge, MA) by incubation at 4 °C for 8 h. After washing three times with PBS containing 0.025% Tween 20 (T-PBS) (pH 7.4), the plate was blocked using bovine serum albumin (BSA) at a concentration of 1 mg/ml in T-PBS at 4 °C for 2.5 h, and then washed again as described above. The MBP-HR1 on the plate was allowed to bind GST-HR2 (50 nM) by incubation at 37 °C for 1.5 h in the presence or absence of various concentrations of compounds for testing. After washing, binding of GST-HR2 was detected by using alkaline phosphatase (ALP)-conjugated anti-GST antibody (Sigma) in 1:2000 dilution at 4 °C for 1 h, then washed as before, prior to the addition of phosphatase substrate 5-bromo-4-chloro-3-indolyl phosphate (BCIP) (BluePhos Microwell Phosphatase Substrate; KPL, Gaithersburg, MD). After incubating at room temperature for 30 min, absorbance at 595 nm was measured by a plate reader (model 3550, Bio-Rad).

### 2.4. Direct detection of interaction of HR1 and HR2 (F-ELISA) (Fig. 2D)

All procedures were performed as described above, except that TRX-ALP-HR2 (50 nM) was used in place of GST-HR2, with binding directly detected by BluePhos Microwell Phosphatase Substrate without the interaction of ALP-conjugated anti-GST antibody.

### 2.5. Anti-HIV activity

Anti-HIV-1 activity was determined by the multinuclear activation of a galactosidase indicator (MAGI) assay as described previously (Kimpton and Emerman, 1992; Kodama et al., 2001). Briefly, the MAGI cells ($10^4$ cells/well) were seeded in flat bottom 96-well microtitre plates. The following day, the cells were inoculated with HIV-1 and cultured in the presence of various concentrations of inhibitors in fresh medium. After 48 h incubation, all the blue cells stained with 5-bromo-4-chloro-3-indolyl-β-D-galactopyranoside (X-gal) in each well were counted.

## 3. Results

### 3.1. Establishment of ELISA

To establish a novel assay system representing the specific interaction of HR1 and HR2 regions of the HIV-1 gp41 protein, a

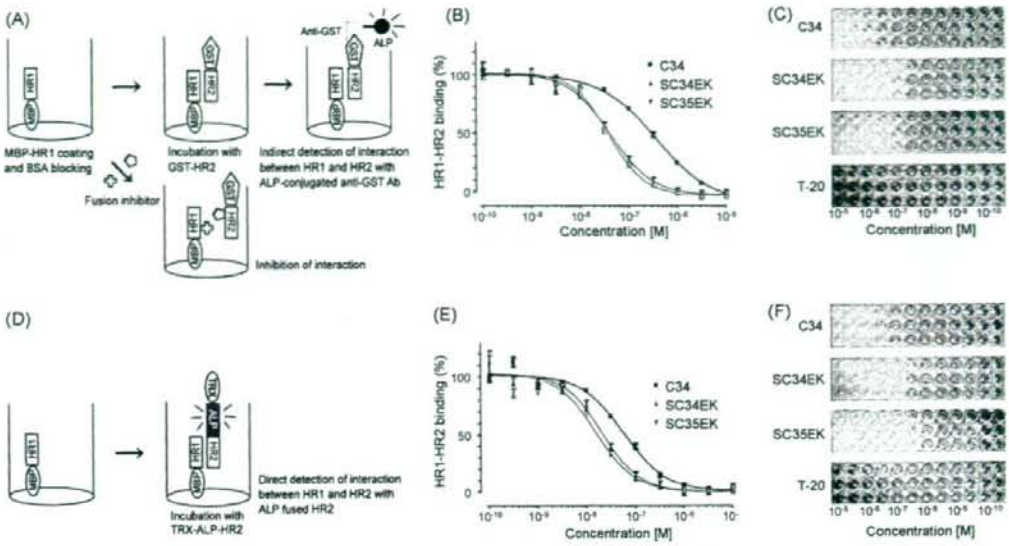


**Fig. 2.** Flow chart of the established ELISA systems (A and D) and the inhibitory effects of peptide-based fusion inhibitors determined by these systems (B, C, E and F). The schemes of Ab-ELISA and F-ELISA are shown. In Ab-ELISA (A), GST-HR2 interacts with MBP-HR1 on the ELISA plate, and the amounts of GST-HR2 are quantified by using ALP-conjugated anti-GST antibody and ALP substrate. In the presence of fusion inhibitors, GST-HR2 cannot interact with MBP-HR1, resulting in no ALP activity. In F-ELISA (D), ALP-fused HR2 protein enables the detection of the interaction of HR2 directly without ALP-conjugated anti-GST antibody. Inhibition curves of binding by Ab-ELISA (B) and F-ELISA (E) at peptide concentrations $10^{-10}$ to $10^{-5}$ M are illustrated. The actual appearance of ELISA plates observed in Ab-ELISA (C) and F-ELISA (F) is shown.

simple ELISA was first established with ALP-conjugated antibody (Ab-ELISA) as shown in Fig. 2A. MBP-HR1 was coated onto a 96-well ELISA plate. After blocking with BSA, GST-HR2 solution was added to the MBP-HR1 coated well. Using ALP-conjugated anti-GST antibody, the interaction of HR1 and HR2 was colorimetrically measured by a plate reader. Agents that block the interaction of HR2 with HR1 can reduce optical density at 595 nm ($OD_{595}$). The period for efficient coating of MBP-HR1 to the plate was measured by detection of ALP-conjugated anti-MBP antibody. After 8 h and up to 24 h little increase in efficiency of MBP-HR1 coating was observed (data not shown). When coating and blocking were performed prior to the assay, total time of the procedure, excluding washing, was only 3 h.

Prior to evaluation of fusion inhibitors, we examined interaction of GST-HR2 with the MBP-HR1 coating. We first coated MBPs with or without HR1 at a concentration of 50 nM, incubated them with various concentrations of GST-HR2, and then detected bound GST-HR2 with anti-GST antibody. GST-HR2 interacted with MBP-HR1 in a dose-dependent manner, at least up to 100 μM and provided sufficient $OD_{595}$ values, over 1.0 (Fig. 3). Thus, 50 nM of GST-HR2 was used for further experiments.

Next, we modified the Ab-ELISA by using ALP-fused HR2 instead of GST-HR2 in the reaction with coated MBP-HR1, as shown in Fig. 2D (F-ELISA). The ALP-fused HR2 enabled us to directly detect the HR1 and HR2 interaction without the antibody reaction step, thus providing an even more rapid and simple procedure than the Ab-ELISA which uses ALP-conjugated antibody for detection. The total time required for the F-ELISA, excluding coating and blocking, was approximately 2 h. These results demonstrate that the ELISA systems detect the interaction of HR1 and HR2 interaction, enables the screening of potential fusion inhibitors without the need for infectious HIV-1 material, and is both simple and rapid.

### 3.2. Inhibitory effect of HR2-derived peptides and other entry inhibitors

The efficacy of the fusion inhibitory peptides C34, SC34EK and SC35EK and other compounds was determined by both Ab-ELISA (Fig. 2A) and F-ELISA (Fig. 2D). Both ELISAs only detected the activities of these three fusion inhibitory peptides, but not of other entry inhibitors (Table 1). The inhibitory effects of these peptide fusion inhibitors were reproducible and displayed a sigmoidal dose-dependent curve (Fig. 2B and E). These results suggested that our established ELISAs were specific for the interaction between HR1 and HR2 in the fusion process. Higher sensitivities for peptides tested were obtained by F-ELISA compared with those by Ab-ELISA (Table 1). However, compared with the MAGI assay, sensitivities of both ELISAs were between 14- and 50-fold lower. Neither ELISA technique was able to detect the inhibitory effect of T-20, which

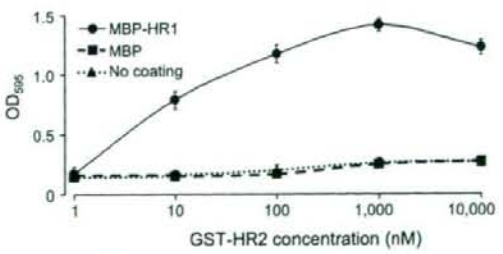


**Fig. 3.** The binding efficacy of GST-HR2. Fifty nanomolars of MBP-HR1 (circle), MBP (square) and mock (triangle with broken line) were coated on the plate. Various concentrations of GST-HR2 were added and incubated at 37 °C for 1.5 h. Bound GST-HR2 was detected with ALP-conjugated anti-GST antibody by measuring the optical density at 595 nm ($OD_{595}$).

**Table 1**
The efficacy of HR2-derived peptides and other entry inhibitors as determined by Ab-ELISA or F-ELISA and the cell-based MAGI assay

| Compounds | $EC_{50}$ (nM)[a] | | | |
|---|---|---|---|---|
| | Ab-ELISA[b] | F-ELISA[c] | MAGI[d] | |
| | | | NL4-3[e] | BaL[f] |
| C34[g] | 365 ± 43 | 59 ± 7.7 | 4.0 ± 0.86 | N.D.[h] |
| SC34EK[g] | 41 ± 5.0 | 21 ± 3.2 | 1.6 ± 0.61 | N.D. |
| SC35EK[g] | 38 ± 3.0 | 16 ± 2.8 | 0.35 ± 0.030 | N.D. |
| T-20[g] | >10,000 | >10,000 | 35 ± 17 | N.D. |
| TAK-779 | >100,000 | >100,000 | >100,000 | 1.85 ± 0.19 |
| AMD-3100 | >100,000 | >100,000 | 0.39 ± 0.030 | >100,000 |
| DS-5000 | >100,000 | >100,000 | 19 ± 6.0 | 348 ± 46 |

[a] $EC_{50}$ refers to the concentration of peptides which show 50% inhibition relative to the control.
[b] The amount of binding GST-HR2 measured by ALP-conjugated anti-GST antibody.
[c] Direct detection of HR1 and HR2 interaction without antibody reaction by using ALP-fused HR2 protein.
[d] Multinuclear activation of a galactosidase indicator assay using HeLa CD4-LTR/β-galactosidase indicator cells (Kimpton and Emerman, 1992).
[e] CXCR4 (X4) tropic HIV-1 strain.
[f] CCR5 (R5) tropic HIV-1 strain.
[g] Peptide sequences are shown in Fig. 1.
[h] Not determined.

has anti-fusion activity in vitro and in vivo, even though the gp41 amino acid region 23–58, which is a predictive site for T-20 interaction, is included in the MBP-HR1 fusion protein (Figs. 1 and 2C and F; Table 1). We further examined the effect on T-20 susceptibility of changing the coating and interaction. In this experiment, first GST-HR2 was coated, then exposed to MBP-HR1, and finally detected by anti-MBP antibody. Again C34 and its derivatives were effective, but T-20 was not (data not shown).

### 3.3. *Effect of DMSO concentration and pH*

For screening, compounds are frequently dissolved in dimethyl sulfoxide (DMSO). However, high concentrations of DMSO (over 1%) reduced cell viability in the cell-based assay, e.g., MAGI assay. The ELISA systems described here do not require cells, thus should be less influenced by DMSO concentration compared to the MAGI assay. To verify this, we determined the concentration of DMSO that affects the interaction of HR1 and HR2 in our ELISAs. In both the Ab-ELISA and F-ELISA, DMSO concentrations up to 10% did not influence the optical densities to any significant extent (Fig. 4A). At these concentrations, optical densities recorded were less than 20% lower compared to those recorded in the absence of DMSO, indicating that the sensitivities of these tests would be sufficient to screen compounds that are dissolved in reagents containing up to 10% DMSO.

Next, we investigated the effect of pH on detection by ELISA. High concentrations of some compounds that are highly acidic or basic may decrease viability of the cells in cell-based assays. The pH of the reaction buffer was modified by addition of HCl and NaOH as control acidic or basic compounds, respectively. In the F-ELISA, binding of HR1 and HR2 was 2–2.5-fold greater at pH less than 7 than at pH 7.4, while in the Ab-ELISA, the binding was relatively stable at pH 6 (Fig. 4B) and reduction of HR1 and HR2 binding was less than 20%. On the other hand, at basic pH, binding of HR1 and HR2 were relatively stable up to pH 9 in both ELISAs. These results indicate that both systems are less influenced by DMSO concentrations up to 10% and in basic reaction conditions compared to cell-based assays. However, in acidic reaction conditions, interaction of HR1 and HR2 is likely to be overestimated in the F-ELISA.

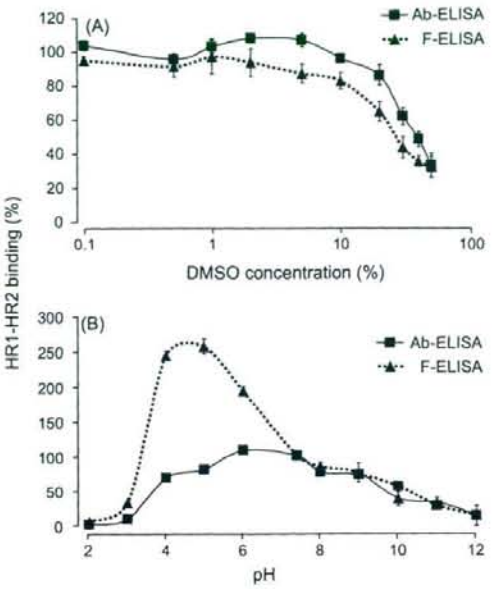


**Fig. 4.** Effects of DMSO concentration and pH. The effect of DMSO from 0.1 to 50% added to the reaction of HR1 and HR2 is shown (A). Binding is expressed as a percentage of that in the absence of DMSO. Alteration of the pH from 2 to 12 at the HR1 and HR2 reaction was performed by using HCl or NaOH (B). Binding is expressed as a percentage of that at pH 7.4.

## 4. Discussion

Our newly established ELISA systems successfully detected the HIV-fusion inhibitory activities of C34, a peptide-based fusion inhibitor (Fig. 1), and its derivatives in a dose-dependent manner. However, T-20 lacking the N-terminal 10 amino acids of C34 but containing an additional 12 amino acids in the C-terminal region did not show activity in either of the ELISA systems (Fig. 2; Table 1). T-20 is believed to inhibit 6-helical bundle formation through competition with the physiological HR2 region of gp41. This hypothesis is strongly supported by the introduction of a site of mutations for T-20 resistance in vivo. Variants isolated from T-20 treated patients frequently display mutations in the HR1 region, especially at amino acids 36–45, including D36G/V/S, V38A/E and N43D (Aquaro et al., 2006; Cabrera et al., 2006; Mink et al., 2005; Poveda et al., 2002; Rimsky et al., 1998; Wei et al., 2002) (Fig. 1). Interestingly, amino acid positions 36–45 are also crucial for C34 binding, and some C34 resistant variants also show cross-resistance to T-20 (Nameki et al., 2005). Moreover, our preliminary data in the time course of addition experiments showed that the profile of inhibition is identical between C34 and T-20 (data not shown).

Our designed MBP-HR1 contains the presumed interaction site of T-20 (amino acid positions 23–58), as determined by crystal structure analysis of the N36–C34 complex (Chan et al., 1997) (Fig. 1). However, we failed to detect T-20 inhibitory activity in our ELISA systems (Fig. 2C and F). To the best of our knowledge, there are no reports that describe the potent activity of T-20 in protein- or peptide-based assays (Cai and Gochin, 2007; Huang et al., 2006, 2007; Jiang et al., 1999; Liu et al., 2007; Ryu et al., 1998; Xu et al., 2007).

In this regard, two groups have tried to reveal the mechanism of action of T-20 mainly through physicochemical experiments, with both groups proposing that T-20 may act through the lipid mem-

brane. Jiang et al. has proposed that HR2 peptides have two different functional domains, an HR1-binding domain, and a lipid-binding domain (Liu et al., 2007). C34 contains an HR1-binding sequence but not a lipid-binding domain, while T-20 has only a lipid-binding domain, suggesting that T-20 might be functional only in the presence of lipid membrane. Wexler-Cohen and Shai (2007), also found that the C-terminal region of T-20 which was not included in C34 could be replaced with fatty acid, indicating that T-20 acts through the lipid membrane.

It is possible that MBP hampers the proper conformation of HR1. However, in the 6-helix bundle crystal structure of human T cell leukemia virus type 1 gp21, MBP remained fused to the N-terminal of HR1 (Kobe et al., 1999). Thus, it is unlikely that the inability of HR1 to bind T-20 is due to improper conformation of HR1. Moreover, even synthetic peptides of HR1 and T-20 do not bind each other (Liu et al., 2005).

To date, several peptide-based detection systems have been reported, although they failed to demonstrate T-20 activity. Most of them utilize the NC-1 monoclonal antibody which recognizes discontinuous epitopes presented on the 6-helix complex between N36 and C34 to detect 6-helical conformations (Huang et al., 2006, 2007; Jiang et al., 1999; Liu et al., 2007). It is predicted that this system may not detect the peptide-based fusion inhibitor C34 itself or may not detect C34 derivatives, since the antibody NC-1 was derived from the 6-helix conformation of N36 and C34 peptides. Ryu et al. (1998) also reported similar ELISA systems, but showed an inhibitory effect only for C51 with an $EC_{50}$ value of 1.0 μg/ml (approximately 200 nM). Other groups have reported the development of assay systems using fluorescence resonance energy transfer (FRET) (Cai and Gochin, 2007; Xu et al., 2007). Although FRET requires no coating and washing steps, it seems to be less sensitive compared to our ELISA systems. In fact, $EC_{50}$ values of C34 in the FRET system were described as approximately 5 μM (Xu et al., 2007), while those in our Ab-ELISA and F-ELISA were 365 and 59 nM, respectively (Table 1).

The sensitivities of our ELISA systems were lower than those of the cell-based MAGI assay (Table 1). However, the ELISA systems could detect the interaction between HR1 and HR2 even at a high concentration of DMSO, and in a relatively wide pH range (Fig. 4), indicating their capacity for screening of highly concentrated compounds. Decreased concentrations of MBP-HR1 and GST-HR2 or ALP-HR2 increased the antiviral sensitivity, although this also reduced detection sensitivity of ALP activity. Detection sensitivity could be increased by using a highly sensitive chemiluminescent probe as an alternative to the BCIP substrate we used.

At pH greater than 8, both ELISAs showed decreased optical density, while at pH less than 7, enhanced ALP activity was observed in F-ELISA compared with the neutral pH 7.4 (Fig. 4B). Although we could not elucidate the detailed mechanism at present, even in Ab-ELISA, the optical density was also enhanced by using an acidic buffer in the incubation of GST-HR2 with anti-GST antibody (data not shown). Thus, low pH enhances ALP activity rather than enhancing the interaction of HR1 and HR2. These results indicate that we should take note of this artificial enhancement when acidic compounds are screened by F-ELISA.

Major difference between class I and class II fusion is based upon the structure of the glycoproteins involved in the fusion process. For instance, HIV and FluV utilize alpha-helix structure domains located in gp41 and HA2, respectively. In contrast, Flaviviruses, which fuse through class II, utilize beta-sheet structure domains in E protein. Although both glycoproteins complete fusion with trimer of hairpins (alpha-helix and beta-sheet, respectively), in the pre-fusion state, they form trimers and dimers, for class I and class II, respectively. Moreover, the fusion peptide domain which is directly inserted into target cell membrane, is located at N-terminus and internal loop of the env-protein, for class I and class II, respectively.

At the virus–cell membrane fusion step, the interaction between viral envelope proteins HR1 and HR2 is a common mechanism of class I fusion (Jahn et al., 2003; Schibli and Weissenhorn, 2004). It is expected that establishment of a similar ELISA screening system for other viruses using class I fusion for cell entry, such as influenza virus (Eckert and Kim, 2001), feline immunodeficiency virus (FIV) (Medinas et al., 2002), severe acute respiratory syndrome coronavirus (SARS-CoV) (Bosch et al., 2004) and Ebola virus (Watanabe et al., 2000) is possible. For some highly virulent agents, such as SARS-CoV and Ebola virus, our system will be an extremely useful tool since it does not require infectious material.

In this study, we have developed two novel in vitro assay systems for fusion inhibitors by focusing on the interaction of envelope proteins HR1 and HR2. Hydrophobic pocket in HR1 and tryptophan rich domain in HR2 acting as "pocket" and "knob", respectively, play a key role in the virus–cell membrane fusion process, indicating that these interactions are an attractive target for small molecule fusion inhibitors (Ferrer et al., 1999). C34, GST-HR2 and ALP-TRX-HR2 used in this study contain "knob" region but T-20 does not. The developed systems are also ideal for initial screenings because of low variability and good reproducibility even at high compound concentration, and since they allow for a non-infectious rapid and simple procedure. These assays will be useful for the discovery of novel fusion inhibitors not only of HIV-1, but also of other viruses which utilize the class I fusion mechanism.

## Acknowledgements

This work was supported in part by grants for the Promotion of AIDS Research from the Ministry of Health and Welfare and the Ministry of Education, Culture, Sports, Science, and Technology of Japan (E.K. and S.O.); a grant for Research for Health Sciences Focusing on Drug Innovation from The Japan Health Sciences Foundation (E.K., S.O., N.F. and M.M.); and the 21st Century COE program "Knowledge Information Infrastructure for Genome Science" (N.F. and H.N.). H.N. is grateful for the JSPS Research Fellowships for Young Scientists. Appreciation is expressed to Mr. Maxwell Reback (Kyoto University) for reading the manuscript.

## References

Aquaro, S., D'Arrigo, R., Svicher, V., Perri, G.D., Caputo, S.L., Visco-Comandini, U., Santoro, M., Bertoli, A., Mazzotta, F., Bonora, S., Tozzi, V., Bellagamba, R., Zaccarelli, M., Narciso, P., Antinori, A., Perno, C.F., 2006. Specific mutations in HIV-1 gp41 are associated with immunological success in HIV-1-infected patients receiving enfuvirtide treatment. J. Antimicrob. Chemother. 58, 714–722.

Baba, M., Nishimura, O., Kanzaki, N., Okamoto, M., Sawada, H., Iizawa, Y., Shiraishi, M., Aramaki, Y., Okonogi, K., Ogawa, Y., Meguro, K., Fujino, M., 1999. A small-molecule, nonpeptide CCR5 antagonist with highly potent and selective anti-HIV-1 activity. Proc. Natl. Acad. Sci. U.S.A. 96, 5698–5703.

Baba, M., Pauwels, R., Balzarini, J., Arnout, J., Desmyter, J., De Clercq, E., 1988. Mechanism of inhibitory effect of dextran sulfate and heparin on replication of human immunodeficiency virus in vitro. Proc. Natl. Acad. Sci. U.S.A. 85, 6132–6136.

Bewley, C.A., Louis, J.M., Ghirlando, R., Clore, G.M., 2002. Design of a novel peptide inhibitor of HIV fusion that disrupts the internal trimeric coiled-coil of gp41. J. Biol. Chem. 277, 14238–14245.

Bosch, B.J., Martina, B.E., Van Der Zee, R., Lepault, J., Haijema, B.J., Versluis, C., Heck, A.J., De Groot, R., Osterhaus, A.D., Rottier, P.J., 2004. Severe acute respiratory syndrome coronavirus (SARS-CoV) infection inhibition using spike protein heptad repeat-derived peptides. Proc. Natl. Acad. Sci. U.S.A. 101, 8455–8460.

Cabrera, C., Marfil, S., García, E., Martinez-Picado, J., Bonjoch, A., Bofill, M., Moreno, S., Ribera, E., Domingo, P., Clotet, B., Ruiz, L., 2006. Genetic evolution of gp41 reveals a highly exclusive relationship between codons 36, 38 and 43 in gp41 under long-term enfuvirtide-containing salvage regimen. AIDS 20, 2075–2080.

Cai, L., Gochin, M., 2007. A novel fluorescence intensity screening assay identifies new low-molecular-weight inhibitors of the gp41 coiled-coil domain of human immunodeficiency virus type 1. Antimicrob. Agents Chemother. 51, 2388–2395.

Calmy, A., Pascual, F., Ford, N., 2004. HIV drug resistance. N. Engl. J. Med. 350, 2720–2721.

Chan, D.C., Fass, D., Berger, J.M., Kim, P.S., 1997. Core structure of gp41 from the HIV envelope glycoprotein. Cell 89, 263–273.
De Clercq, E., Yamamoto, N., Pauwels, R., Balzarini, J., Witvrouw, M., De Vreese, K., Debyser, Z., Rosenwirth, B., Peichl, P., Datema, R., et al., 1994. Highly potent and selective inhibition of human immunodeficiency virus by the bicyclam derivative JM3100. Antimicrob. Agents Chemother. 38, 668–674.
Dodt, J., Schmitz, T., Schäfer, T., Bergmann, C., 1986. Expression, secretion and processing of hirudin in *E. coli* using the alkaline phosphatase signal sequence. FEBS Lett. 202, 373–377.
Eckert, D.M., Kim, P.S., 2001. Mechanisms of viral membrane fusion and its inhibition. Annu. Rev. Biochem. 70, 777–810.
Fätkenheuer, G., Pozniak, A.L., Johnson, M.A., Plettenberg, A., Staszewski, S., Hoepelman, A.I., Saag, M.S., Goebel, F.D., Rockstroh, J.K., Dezube, B.J., Jenkins, T.M., Medhurst, C., Sullivan, J.F., Ridgway, C., Abel, S., James, I.T., Youle, M., van der Ryst, E., 2005. Efficacy of short-term monotherapy with maraviroc, a new CCR5 antagonist, in patients infected with HIV-1. Nat. Med. 11, 1170–1172.
Ferrer, M., Kapoor, T.M., Strassmaier, T., Weissenhorn, W., Skehel, J.J., Oprian, D., Schreiber, S.L., Wiley, D.C., Harrison, S.C., 1999. Selection of gp41-mediated HIV-1 cell entry inhibitors from biased combinatorial libraries of non-natural binding elements. Nat. Struct. Biol. 6, 953–960.
Frey, G., Rits-Volloch, S., Zhang, X.Q., Schooley, R.T., Chen, B., Harrison, S.C., 2006. Small molecules that bind the inner core of gp41 and inhibit HIV envelope-mediated fusion. Proc. Natl. Acad. Sci. U.S.A. 103, 13938–13943.
Grinsztejn, B., Nguyen, B.Y., Katlama, C., Gatell, J.M., Lazzarin, A., Vittecoq, D., Gonzalez, C.J., Chen, J., Harvey, C.M., Isaacs, R.D., 2007. Safety and efficacy of the HIV-1 integrase inhibitor raltegravir (MK-0518) in treatment-experienced patients with multidrug-resistant virus: a phase II randomised controlled trial. Lancet 369, 1261–1269.
Hazuda, D.J., Young, S.D., Guare, J.P., Anthony, N.J., Gomez, R.P., Wai, J.S., Vacca, J.P., Handt, L., Motzel, S.L., Klein, H.J., Dornadula, G., Danovich, R.M., Witmer, M.V., Wilson, K.A., Tussey, L., Schleif, W.A., Gabryelski, L.S., Jin, L., Miller, M.D., Casimiro, D.R., Emini, E.A., Shiver, J.W., 2004. Integrase inhibitors and cellular immunity suppress retroviral replication in rhesus macaques. Science 305, 528–532.
Huang, J.H., Liu, Z.Q., Liu, S., Jiang, S., Chen, Y.H., 2006. Identification of the HIV-1 gp41 core-binding motif—HXXNPF. FEBS Lett. 580, 4807–4814.
Huang, J.H., Yang, H.W., Liu, S., Li, J., Jiang, S., Chen, Y.H., 2007. The mechanism by which molecules containing the HIV gp41 core-binding motif HXXNPF inhibit HIV-1 envelope glycoprotein-mediated syncytium formation. Biochem. J. 403, 565–571.
Jahn, R., Lang, T., Südhof, T.C., 2003. Membrane fusion. Cell 112, 519–533.
Jiang, S., Lin, K., Zhang, L., Debnath, A.K., 1999. A screening assay for antiviral compounds targeted to the HIV-1 gp41 core structure using a conformation-specific monoclonal antibody. J. Virol. Methods 80, 85–96.
Kikuchi, Y., Yoda, K., Yamasaki, M., Tamura, G., 1981. The nucleotide sequence of the promoter and the amino-terminal region of alkaline phosphatase structural gene (phoA) of *Escherichia coli*. Nucl. Acids Res. 9, 5671–5678.
Kimpton, J., Emerman, M., 1992. Detection of replication-competent and pseudotyped human immunodeficiency virus with a sensitive cell line on the basis of activation of an integrated beta-galactosidase gene. J. Virol. 66, 2232–2239.
Kobe, B., Center, R.J., Kemp, B.E., Poumbourios, P., 1999. Crystal structure of human T cell leukemia virus type 1 gp21 ectodomain crystallized as a maltose-binding protein chimera reveals structural evolution of retroviral transmembrane proteins. Proc. Natl. Acad. Sci. U.S.A. 96, 4319–4324.
Kodama, E.I., Kohgo, S., Kitano, K., Machida, H., Gatanaga, H., Shigeta, S., Matsuoka, M., Ohrui, H., Mitsuya, H., 2001. 4′-Ethynyl nucleoside analogs: potent inhibitors of multidrug-resistant human immunodeficiency virus variants in vitro. Antimicrob. Agents Chemother. 45, 1539–1546.
Lalezari, J.P., Henry, K., O'Hearn, M., Montaner, J.S., Piliero, P.J., Trottier, B., Walmsley, S., Cohen, C., Kuritzkes, D.R., Eron Jr., J.J., Chung, J., DeMasi, R., Donatacci, L., Drobnes, C., Delehanty, J., Salgo, M., 2003. Enfuvirtide, an HIV-1 fusion inhibitor, for drug-resistant HIV infection in North and South America. N. Engl. J. Med. 348, 2175–2185.
Lazzarin, A., Clotet, B., Cooper, D., Reynes, J., Arasteh, K., Nelson, M., Katlama, C., Stellbrink, H.J., Delfraissy, J.F., Lange, J., Huson, L., DeMasi, R., Wat, C., Delehanty, J., Drobnes, C., Salgo, M., 2003. Efficacy of enfuvirtide in patients infected with drug-resistant HIV-1 in Europe and Australia. N. Engl. J. Med. 348, 2186–2195.
Liu, S., Jing, W., Cheung, B., Lu, H., Sun, J., Yan, X., Niu, J., Farmar, J., Wu, S., Jiang, S., 2007. HIV gp41 C-terminal heptad repeat contains multifunctional domains. Relation to mechanisms of action of anti-HIV peptides. J. Biol. Chem. 282, 9612–9620.
Liu, S., Lu, H., Niu, J., Xu, Y., Wu, S., Jiang, S., 2005. Different from the HIV fusion inhibitor C34, the anti-HIV drug Fuzeon (T-20) inhibits HIV-1 entry by targeting multiple sites in gp41 and gp120. J. Biol. Chem. 280, 11259–11273.
Medinas, R.J., Lambert, D.M., Tompkins, W.A., 2002. C-terminal gp40 peptide analogs inhibit feline immunodeficiency virus: cell fusion and virus spread. J. Virol. 76, 9079–9086.
Mink, M., Mosier, S.M., Janumpalli, S., Davison, D., Jin, L., Melby, T., Sista, P., Erickson, J., Lambert, D., Stanfield-Oakley, S.A., Salgo, M., Cammack, N., Matthews, T., Greenberg, M.L., 2005. Impact of human immunodeficiency virus type 1 gp41 amino acid substitutions selected during enfuvirtide treatment on gp41 binding and antiviral potency of enfuvirtide in vitro. J. Virol. 79, 12447–12454.
Nameki, D., Kodama, E., Ikeuchi, M., Mabuchi, N., Otaka, A., Tamamura, H., Ohno, M., Fujii, N., Matsuoka, M., 2005. Mutations conferring resistance to human immunodeficiency virus type 1 fusion inhibitors are restricted by gp41 and Rev-responsive element functions. J. Virol. 79, 764–770.
Otaka, A., Nakamura, M., Nameki, D., Kodama, E., Uchiyama, S., Nakamura, S., Nakano, H., Tamamura, H., Kobayashi, Y., Matsuoka, M., Fujii, N., 2002. Remodeling of gp41-C34 peptide leads to highly effective inhibitors of the fusion of HIV-1 with target cells. Angew. Chem. Int. Ed. Engl. 41, 2937–2940.
Poveda, E., Rodés, B., Toro, C., Martín-Carbonero, L., Gonzalez-Lahoz, J., Soriano, V., 2002. Evolution of the gp41 env region in HIV-infected patients receiving T-20, a fusion inhibitor. AIDS 16, 1959–1961.
Rimsky, L.T., Shugars, D.C., Matthews, T.J., 1998. Determinants of human immunodeficiency virus type 1 resistance to gp41-derived inhibitory peptides. J. Virol. 72, 986–993.
Root, M.J., Kay, M.S., Kim, P.S., 2001. Protein design of an HIV-1 entry inhibitor. Science 291, 884–888.
Ryu, J.R., Lee, J., Choo, S., Yoon, S.H., Woo, E.R., Yu, Y.G., 1998. Development of an in vitro assay system for screening of gp41 inhibitory compounds. Mol. Cells 8, 717–723.
Schibli, D.J., Weissenhorn, W., 2004. Class I and class II viral fusion protein structures reveal similar principles in membrane fusion. Mol. Membr. Biol. 21, 361–371.
Tagat, J.R., McCombie, S.W., Nazareno, D., Labroli, M.A., Xiao, Y., Steensma, R.W., Strizki, J.M., Baroudy, B.M., Cox, K., Lachowicz, J., Varty, G., Watkins, R., 2004. Piperazine-based CCR5 antagonists as HIV-1 inhibitors. IV. Discovery of 1-[(4,6-dimethyl-5-pyrimidinyl)carbonyl]-4-[4-[2-methoxy-1(*R*)-4-(trifluoromethyl)phenyl]ethyl-3(*S*)-methyl-1-piperazinyl]-4-methylpiperidine (Sch-417690/Sch-D), a potent, highly selective, and orally bioavailable CCR5 antagonist. J. Med. Chem. 47, 2405–2408.
Watanabe, S., Takada, A., Watanabe, T., Ito, H., Kida, H., Kawaoka, Y., 2000. Functional importance of the coiled-coil of the Ebola virus glycoprotein. J. Virol. 74, 10194–10201.
Wei, X., Decker, J.M., Liu, H., Zhang, Z., Arani, R.B., Kilby, J.M., Saag, M.S., Wu, X., Shaw, G.M., Kappes, J.C., 2002. Emergence of resistant human immunodeficiency virus type 1 in patients receiving fusion inhibitor (T-20) monotherapy. Antimicrob. Agents Chemother. 46, 1896–1905.
Wexler-Cohen, Y., Shai, Y., 2007. Demonstrating the C-terminal boundary of the HIV 1 fusion conformation in a dynamic ongoing fusion process and implication for fusion inhibition. FASEB J. 21, 3677–3684.
Xu, Y., Hixon, M.S., Dawson, P.E., Janda, K.D., 2007. Development of a FRET assay for monitoring of HIV gp41 core disruption. J. Org. Chem. 72, 6700–6707.

The International Journal of Biochemistry & Cell Biology 40 (2008) 2410–2420

Contents lists available at ScienceDirect

The International Journal of Biochemistry & Cell Biology

journal homepage: www.elsevier.com/locate/biocel

# 2′-Deoxy-4′-C-ethynyl-2-halo-adenosines active against drug-resistant human immunodeficiency virus type 1 variants

Atsushi Kawamoto[a], Eiichi Kodama[a,*], Stefan G. Sarafianos[b], Yasuko Sakagami[a], Satoru Kohgo[c], Kenji Kitano[c], Noriyuki Ashida[c], Yuko Iwai[c], Hiroyuki Hayakawa[c], Hirotomo Nakata[d,e], Hiroaki Mitsuya[d,e], Eddy Arnold[f], Masao Matsuoka[a]

[a] Laboratory of Virus Immunology, Institute for Virus Research, Kyoto University, 53 Kawaramachi, Shogoin, Sakyo-ku, Kyoto 606-8507, Japan
[b] Department of Molecular Microbiology and Immunology, University of Missouri-Columbia, School of Medicine and Christopher S. Bond Life Sciences Center, Columbia, MO 65211, USA
[c] Biochemicals Division, Yamasa Corporation, Chiba 288-0056, Japan
[d] Department of Hematology and Infectious Diseases, Kumamoto University School of Medicine, Kumamoto 860-8556, Japan
[e] Experimental Retrovirology Section, HIV and AIDS Malignancy Branch, National Cancer Institute, Bethesda, MD 20892, USA
[f] Center for Advanced Biotechnology and Medicine and Department of Chemistry and Chemical Biology, Rutgers University, Piscataway, NJ 08854, USA

ARTICLE INFO

*Article history:*
Received 3 December 2007
Received in revised form 14 March 2008
Accepted 2 April 2008
Available online 11 April 2008

*Keywords:*
Human immunodeficiency virus
Reverse transcriptase inhibitor
Resistance

ABSTRACT

One of the formidable challenges in therapy of infections by human immunodeficiency virus (HIV) is the emergence of drug-resistant variants that attenuate the efficacy of highly active antiretroviral therapy (HAART). We have recently introduced 4′-ethynyl-nucleoside analogs as nucleoside reverse transcriptase inhibitors (NRTIs) that could be developed as therapeutics for treatment of HIV infections. In this study, we present 2′-deoxy-4′-C-ethynyl-2-fluoroadenosine (EFdA), a second generation 4′-ethynyl inhibitor that exerted highly potent activity against wild-type HIV-1 ($EC_{50}$ ~ 0.07 nM). EFdA retains potency toward many HIV-1 resistant strains, including the multi-drug resistant clone HIV-$1_{A62V/V75I/F77L/F116Y/Q151M}$. The selectivity index of EFdA (cytotoxicity/inhibitory activity) is more favorable than all approved NRTIs used in HIV therapy. Furthermore, EFdA efficiently inhibited clinical isolates from patients heavily treated with multiple anti-HIV-1 drugs. EFdA appears to be primarily phosphorylated by the cellular 2′-deoxycytidine kinase (dCK) because: (a) the antiviral activity of EFdA was reduced by the addition of dC, which competes nucleosides phosphorylated by the dCK pathway, (b) the antiviral activity of EFdA was significantly reduced in dCK-deficient HT-1080/Ara-C$^r$ cells, but restored after dCK transduction. Further, unlike other dA analogs, EFdA is completely resistant to degradation by adenosine deaminase. Moderate decrease in susceptibility to EFdA is conferred by a combination of three RT mutations (I142V, T165R, and M184V) that result in a significant decrease of viral fitness. Molecular modeling analysis suggests that the M184V/I substitutions may reduce anti-HIV activity of EFdA through steric hindrance between its 4′-ethynyl moiety and the V/I184 β-branched side chains. The present data suggest that EFdA, is a promising candidate for developing as a therapeutic agent for the treatment of individuals harboring multi-drug resistant HIV variants.



## 1. Introduction

Highly active antiretroviral therapies (HAART), combining two or more reverse transcriptase inhibitors (RTIs) and/or protease inhibitors, have been successful in sig-

* Corresponding author. Tel.: +81 75 751 3986; fax: +81 75 751 3986.
*E-mail address:* ekodama@virus.kyoto-u.ac.jp (E. Kodama).

1357-2725/$ – see front matter © 2008 Elsevier Ltd. All rights reserved.
doi:10.1016/j.biocel.2008.04.007

nificantly reducing viral loads and bringing about clinical benefits to the treatment of patients infected with human immunodeficiency virus type 1 (HIV-1). Although HAART improves prognosis for HIV-1 infected patients (Palella et al., 1998), drug-resistant viruses emerge during prolonged therapy and some resistant viruses show intra-class cross resistance. Moreover, drug-resistant variants can be transmitted to other individuals as primary infections (Little et al., 2002). Hence, there is a great need for the development of new HIV inhibitors that retain activity against drug-resistant HIV variants.

In this regard, we have focused on the family of nucleoside reverse transcriptase inhibitors (NRTIs) and have previously reported that a series of 2′-deoxy-4′-C-ethynyl-nucleosides (EdNs) efficiently suppress ($EC_{50}$s as low as one nanomolar) various NRTI-resistant HIV strains including multi-drug resistant clinical isolates (Kodama et al., 2001). More recently, Haraguchi and others have reported that additional members of EdNs such as 2′,3′-didehydro-3′-deoxy-4′-C-ethynyl-thymidine (Ed4T) are also active against wild-type and drug-resistant strains ($EC_{50}$s ranged from 0.16 to 17 μM) and less toxic than d4T (also known as stavudine) *in vitro* (Dutschman et al., 2004; Haraguchi et al., 2003), while 4′-Ed4T is only moderately active against (−)-2′,3′-dideoxy-3′-thiacytidine (3TC or lamivudine)-resistant HIV-$1_{M184V}$ (Nitanda et al., 2005).

To further increase the antiviral activity and reduce the cytotoxicity, we designed and synthesized a second generation of 4′-substituted adenosine analogs with halogen substitutions at their 2-position. We report here that 2′-deoxy-4′-C-ethynyl-2-fluoroadenosine (EFdA) exhibits the highest antiviral activity than any other NRTI when assayed against wild-type or NRTI-resistant HIV clones and clinical isolates from patients treated extensively with anti-HIV agents. In addition, unlike other adenosine-based NRTIs, EFdA showed adenosine deaminase (ADA) resistance. We also show that EFdA is primarily activated through phosphorylation by cellular deoxycytidine kinase (dCK). Molecular modeling analysis has been used to rationalize the resistance profile of these analogs toward key NRTI mutations.

## 2. Materials and methods

### 2.1. Compounds

3′-Azido-3′-deoxythymidine (AZT, or zidovudine), 2′,3′-dideoxyinosine (ddI, or didanosine), and 2′,3′-dideoxycytidine (ddC, or zalcitabine) were purchased from Sigma (St. Louis, MO.). 3TC was kindly provided from S. Shigeta (Fukushima Medical University, Fukushima, Japan). A set of EdN analogs were designed and synthesized as described elsewhere (Ohrui, 2006). Their chemical structures are shown in Fig. 1. 2′-Deoxycoformycin (dCF) was synthesized in Yamasa Corporation (Choshi, Japan).

### 2.2. Cells and plasmids

MT-2 and MT-4 cells were grown in an RPMI 1640-based culture medium, and 293T cells were grown in Dulbecco's modified Eagle medium (DMEM); each of these media was

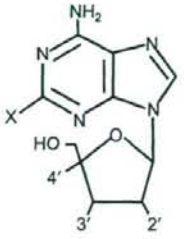


| Base X | Sugar 2′ | Sugar 3′ | 4′ | Compound abbreviation |
|---|---|---|---|---|
| -H | -H | -OH | -C ≡ CH | *E*dA |
| -F | -H | -OH | -C ≡ CH | 2F-*E*dA |
| -F | -H | -H | -C ≡ CH | 2F-*E*ddA |
| -F | C = C | | -C ≡ CH | 2F-*E*d4A |
| -F | -H | -OH | -C ≡ N | 2F-CNdA |
| -Cl | -H | -OH | -C ≡ CH | 2Cl-*E*dA |

**Fig. 1.** Structures of 4′-substituted adenosine analogs. All nucleoside analogs discussed here have substitutions at the 4′-position of the sugar ring.

supplemented with 10% fetal calf serum (FCS), 2 mM L-glutamine, 100 U/ml penicillin, and 50 μg/ml streptomycin. HeLa-CD4-LTR/β-galactosidase (MAGI) cells were propagated in DMEM supplemented with 10% FCS, 0.2 mg/ml of hygromycin B, and 0.2 mg/ml of G418 (Kimpton and Emerman, 1992). HeLa-CD4/CCR5-LTR/β-galactosidase cells were propagated in puromycin (10 μg/ml) containing DMEM with hygromycin and G418. Peripheral blood mononuclear cells (PBMCs) were obtained from healthy HIV-1-seronegative donors by Ficoll-Hypaque gradient centrifugation and stimulated for 3 days with phytohemagglutinin M (PHA; 10 μg/ml; Sigma) and recombinant human interleukin 2 (IL-2; 10 U/ml; Shionogi & Co., Ltd., Osaka, Japan) prior to use. Human fibrosarcoma cell lines, HT-1080 and HT-1080/Ara-$C^r$ were grown in the RPMI-based culture medium (Obata et al., 2001). To express HIV-1 receptors, we constructed a mammalian expression vector pBC-CD4/CXCR4-IH, which encodes CD4, CXCR4, and hygromycin phosphotransferase with two internal ribosome entry sites under control of cytomegalovirus promoter as described (Kajiwara et al., 2006). After the transfection into HT-1080 and HT-1080/Ara-$C^r$, cells were selected by 0.2 mg/ml hygromycin B. For the expression of human deoxycytidine kinase (dCK), pCI-neo (Promega, Madison, WI)-based plasmid, pCI-dCK, was transfected into HT-1080/Ara-$C^r$ and selected with 0.2 mg/ml G418. Established cells were designated HT-1080/Ara-$C^r$/dCK. Puromycin resistance gene under the control of PGK promoter was inserted into pLTR-SEAP (Miyake et al., 2003), which encodes a secreted form of the placental alkaline phosphatase (SEAP) gene under control of the HIV-1 long terminal repeat (LTR) (pLTR-SEAP-puro$^r$). pLTR-SEAP-puro$^r$ was transfected into the three HT-1080 cell lines and selected with 10 μg/ml puromycin.

### 2.3. Viruses and construction of recombinant HIV-1 clones

Two laboratory strains, HIV-$1_{IIIB}$ and HIV-$2_{EHO}$, were used. Multi-drug resistant clinical HIV-1 strains, which had been exposed to over 10 anti-HIV-1 drugs for at least 3 years, were passaged in PHA-stimulated PBMCs (PHA-PBMCs) and stored at −80 °C until further use. Recombinant infectious HIV-1 clones carrying various mutations in the *pol* gene were generated using pNL101 (Jeang et al., 1993). Briefly, desired mutations were introduced into the XmaI–NheI region (759 bp) of pTZNX1, which encoded Gly-15 to Ala-267 of HIV-1 RT (strain BH 10) by a site-directed mutagenesis method (Weiner et al., 1994). The XmaI–NheI fragment was inserted into a pNL101-based plasmid, pNL-RT, generating various molecular clones with the desired mutations. To generate pNL-RT, we first introduced a silent mutation at NheI site of the pNL101, GCTAGC to GCCAGC (underlined; 7251 n.t. from the 5′-LTR) by site-directed mutagenesis. Then, the ApaI–SalI fragment of pNL101 without the NheI site was replaced with that of pSUM9 (Shirasaka et al., 1995), to introduce XmaI and NheI site in the RT coding region. The presence of intended substitutions and the absence of unintended substitutions in the molecular clones were confirmed by sequencing. Each molecular clone (2 μg/ml as DNA) was transfected into 293T cells ($4 \times 10^5$ cells/6-well plate) by FuGENE 6 Transfection Reagent (Roche Diagnostics, Indianapolis, IN). After 24 h, MT-2 cells ($10^6$ cells/well) were added and co-cultured with 293T cells for an additional 24 h. When an extensive cytopathic effect was observed, the cell supernatants were harvested, and the virus was further propagated in MT-4 cells. The culture supernatant was harvested and stored at −80 °C until further use.

### 2.4. Determination of drug susceptibility

The inhibitory effect of test compounds on viral replication for 5 days was evaluated in MT-4 cells by the MTT method as described previously (Kodama et al., 2001). The sensitivity of NRTI-resistant infectious clones to test compounds was determined by the MAGI assay as described (Nameki et al., 2005). The drug susceptibility of HIV-1 clinical isolates was determined on day 7 by a commercially available p24 antigen assay (Kodama et al., 2001). Briefly, PHA-PBMCs ($10^6$ cells/ml) were exposed to each viral preparation at $TCID_{50}$ of 50 and cultivated in 200 μl of culture medium containing various concentration of the drug in 96-well culture plates. All assays were performed in triplicate, and the amounts of p24 antigen produced by the cells into the culture medium were determined. A 2′-deoxynucleoside competition assay was performed by the same way as the MAGI assay. An adenosine deaminase (ADA) inhibitor, dCF, was added for preventing conversion of 2′-deoxyadenosine (dA) to 2′-deoxyinosine (dI) (final concentration 0.4 μM). The effect of dCK expression on activities of test compounds was examined by measurement of SEAP activity in the supernatant. At first, the target cells (HT-1080, HT-1080/Ara-$C^r$, and HT-1080/Ara-$C^r$/dCK) were suspended in 96-well plates ($5.0 \times 10^3$ cells/well). On the following day, the cells were inoculated with HIV-$1_{IIIB}$ (500 MAGI unit/well, giving 500 blue cells in MAGI cells) in the presence of serially diluted compounds. After 48 h incubation, supernatant was collected and SEAP activity in the supernatant was measured using BD Great EscAPe SEAP chemiluminescence detection kit (BD Biosciences Clontech., Palo Alto, CA) and Wallac 1450 MicroBeta Jet Luminometer (PerkinElmer, Wellesley, MA).

### 2.5. The effect of ADA

The effect of ADA on EdA or EFdA was examined by high performance liquid chromatography (HPLC). ADA (0.01 U) derived from bovine intestinal tract was added into 0.5 ml of 0.5 mM EFdA in 50 mM Tris–HCl buffer (pH 7.5), and incubated at 25 °C. Samples were collected each 15 min and analyzed by HPLC.

### 2.6. HIV-1 replication assays

MT-2 cells ($2.5 \times 10^5$ cells/5 ml) were infected with each virus preparation (500 MAGI units) for 4 h. The infected cells were then washed and cultured in a final volume of 5 ml. Culture supernatants (200 μl) were harvested from days 1 to 7 after infection, and the p24 antigen amounts were quantified (Nameki et al., 2005).

For competitive HIV-1 replication assay (CHRA), two titrated infectious clones to be examined were mixed and added to MT-2 cells ($10^5$ cells/3 ml) as described previously (Kosalaraksa et al., 1999; Nameki et al., 2005). To ensure that the two infectious clones being compared were of approximately equal infectivity, a fixed amount (500 MAGI units) of one infectious clone was mixed with three different amounts (250, 500 and 1000 MAGI units) of the other infectious clone. On day 1, one-third of the infected MT-2 cells were harvested, washed twice with phosphate-buffered saline, and the cellular DNA was extracted. The purified DNA was subjected to nested PCR and then direct DNA sequencing. The HIV-1 coculture which best approximated a 50:50 mixture on day 1 was further propagated. Every 4–6 days, the cell-free supernatant of the virus coculture (1 ml) was transmitted to new uninfected MT-2 cells. The cells harvested at the end of each passage were subjected to direct sequencing, and the viral population change was determined by the relative peak height in the sequencing chromatogram. The persistence of the original amino acid substitution was confirmed in all infectious clones used in this assay.

### 2.7. Molecular modeling studies

The programs SYBYL and O were used to prepare models of the complexes of wild-type, M184V, and insertion mutant HIV-1 RT with DNA and the triphosphates of 3TC and EFdA. The starting atomic coordinates of HIV-1 RT were from the structure described by Huang et al. (PDB code 1RTD) (Huang et al., 1998). The side-chain mutations were manually modeled using mostly conformations encountered in RT structures that carry such mutations. The local structures of mutants were optimized using energy minimization protocols in SYBYL. The triphosphates of the inhibitors were built based on the structures of dTTP in